



# Vibration analysis of variable thickness functionally graded toroidal shell segments

Pham Minh Vuong<sup>1</sup> · Nguyen Dinh Duc<sup>2</sup>

Received: 27 February 2023 / Revised: 23 June 2023 / Accepted: 2 July 2023 / Published online: 19 July 2023  
© Wrocław University of Science and Technology 2023

## Abstract

In this paper, for the first time, the nonlinear vibration response of toroidal shell segments with varying thickness subjected to external pressure is investigated analytically using Reddy's third-order shear deformation shell theory. The variable thickness shells are made of functionally graded material (FGM) that is created from ceramic and metal constituents. The material properties of FGM shells are assumed to be gradually graded in the thickness direction according to a simple power-law distribution in terms of volume fractions of constituents. Equations of motion of variable thickness FGM toroidal shell segments are established based on Reddy's third-order shear deformation shell theory with von Kármán nonlinearity. The Galerkin method and the Runge–Kutta method are used to solve the governing system of partial differential equations of motion, and then the nonlinear vibration response of variable thickness FGM toroidal shell segment is analyzed. A numerical analysis is also performed to show the effects of material and geometrical parameters on the nonlinear vibration response of variable thickness FGM toroidal shell segments.

**Keywords** Variable thickness FGM toroidal shell segment · Nonlinear vibration · Reddy's third-order shear deformation shell theory · von Kármán nonlinearity

## 1 Introduction

In recent years, the study on the stability and vibration of thin structural components with variable thickness has attracted many researchers' interests. Irie et al. [1] and Efraim and Eisenberger [2] studied vibration of variable thickness annular plate and variable thickness thick FGM plates, respectively. Based on classical shell theory, Koiter et al. [3] studied the buckling of cylindrical shells with small periodic axisymmetric thickness variations under axial compression using the energy criterion and a modified shooting method. The buckling of a cylindrical shell with small thickness variations subjected to external pressure has been studied by Nguyen et al. [4] making use of the

perturbation technique and the Bubnov–Galerkin method. Li et al. [5] investigated the effect of thickness variation on the stability of composite cylindrical shells subjected to axial compressive load using the perturbation technique and weighted residuals method based on classical shell theory. Also, based on classical shell theory, buckling of a cylindrical shell with variable thickness under axial compression is investigated by Brar et al. [6] making use of the finite difference method. Chen et al. [7] and Feng et al. [8] made use of the perturbation technique, the Galerkin method, and classical shell theory to investigate the buckling of cylindrical shells with arbitrary axisymmetric variable thickness under axial compression and the buckling of pressure loaded cylindrical shells with arbitrary circumferential thickness variations, respectively. Zhou et al. [9] studied the buckling of a cylindrical shell with stepwise variable thickness under external pressure using the hybrid perturbation–Galerkin method. Free vibration characteristics of rotating cylindrical shells with variable thickness is studied by Taati et al. [10] using Galerkin method. Duan and Koh [11] used an analytical approach to investigate free vibration of variable thickness cylindrical shells. A semi-analytical finite element approach is used by Ganesan and Sivadas [12], and Sivadas

✉ Nguyen Dinh Duc  
ducnd@vnu.edu.vn

<sup>1</sup> Faculty of Civil and Industrial, Hanoi University of Civil Engineering, 55 Giai Phong Street, Hai Ba Trung District, Hanoi, Vietnam

<sup>2</sup> Faculty of Civil Engineering, VNU Hanoi-University of Engineering and Technology, 144 Xuan Thuy Street, Cau Giay District, Hanoi, Vietnam

and Ganesan [13] to investigate the free vibration behaviour of isotropic circular cylindrical shells and cantilever isotropic circular cylindrical shells with thickness varied in the axial direction, respectively. Using Wittrick-Williams algorithm, El-Kaabazi and Kennedy [14] studied free vibration of variable thickness cylindrical shell. Viswanathan et al. [15] made use of the Spline Function approximation and a point collocation method to study free vibration of layered circular cylindrical with variable thickness. Based on classical shell theory, Aksogan and Sofiyev [16] used the Galerkin method and the Ritz method to investigate the dynamic buckling of a cylindrical shell with variable thickness loaded by a uniform external pressure. Jia-chu et al. [17], and Xin-zhi et al. [18] studied stability, and natural frequency of variable thickness conical shells, respectively.

All the above-mentioned studies are based on classical thin shell theory, usually used for static and dynamic analysis of thin-shell structures. Higher order shear deformation theory has been used for investigating the static and dynamic behaviour of thicker structures with variable thicknesses. Kalbaran and Kurtaran [19] based on the first-order shear deformation shell theory to study the nonlinear static response of laminated composite elliptic panels having variable thickness using the generalized differential quadrature method and Newton–Raphson method. Also, based on the first-order shear deformation shell theory, Nasrekani and Eipakchi [20], and Eipakchi and Nasrekani [21] investigated the displacements of isotropic cylindrical shells and auxetic composite cylindrical shells with variable thickness under external pressure and axial compressive load using the perturbation technique, respectively. Duc et al. [22] made use of the first-order shear deformation shell theory to investigate vibration and dynamic response of sandwich panel with variable thickness.

Functionally graded materials (FGMs) are known as advanced materials usually composed of metal and ceramic constituents, in which material properties gradually vary from one interface to the other. In recent years, static and dynamic behaviours of FGM structures, especially variable thickness FGM structures, have received attention. Shariyat and Alipour [23] presented an analytical approach to investigate the bending and stress of FGM auxetic conical/cylindrical shells with variable thickness based on the first-order shear deformation shell theory. Khoshgoftar [24] and Khoshgoftar et al. [25] used the total potential energy approach and perturbation method to analyze the static behaviour of cylindrical shells with variable thickness based on the first-order shear deformation shell theory and the second-order shear deformation shell theory, respectively. Based on the first-order shear deformation shell theory and perturbation technique, Parhizkar Yaghoobi and Ghannad [26] studied static behaviour of variable thickness FGM cylindrical shell

under thermal load. Kashkoli et al. [27] made use of multi-layer method to study static response of FGM cylindrical shell with variable thickness loaded by thermo-mechanical loads. Saeedi et al. [28] investigated static response of long FGM cylindrical shell under thermomechanical loading using the differential quadrature method. Also, using the differential quadrature method, Behravan Rad and Shariyat [29] static response of variable thickness annular plates subjected to magnetic, thermal, and mechanical loads.

Hayati and Atai [30] based on a third-order shear deformation shell theory to study multiobjective mechanical buckling optimization FGM cylindrical shell with thickness variation and initial imperfection, making use of energy approach and finite element modes. Also, using finite element model, Minh and Duc [31] studied the effects of cracks on the stability of variable thickness FGM plates based on the phase-field theory and the new third-order shear deformation plate theory. Using the differential quadrature method, Akbari Alashti and Ahmadi [32] studied buckling of variable thickness FGM cylindrical shell loaded by axial compression and external pressure.

Kim et al. [33] based on the first-order shear deformation shell theory to investigate vibration of FGM doubly curved shell of revolution by using a semi-analytical method. Phu et al. [34] studied nonlinear dynamics responses of variable thickness FGM cylinder shell based on classical thin shell theory. Quoc et al. [35] based on the first-order shear deformation shell theory and Galerkin method investigated vibration of rotating FGM cylindrical shell with variable thickness. Miao et al. [36] investigated free vibration of variable thickness 2D-FGMs cylindrical shell making use of the Sanders' shell theory, Chebyshev polynomials and the Rayleigh–Ritz method. Ahlawat and Saini [37] studied vibration and buckling of 2D-FGM circular plates with variable thickness using Hamilton's principle and the Harmonic differential quadrature method. Based on the first-order shear deformation shell theory, Kurpa et al. [38] investigated vibration of variable thickness FGM shallow shells making use of R-functions method.

Toroidal shell segments are special structures and have found applications in practical. Studies on the buckling, postbuckling, and vibration of toroidal shell segments in general, and toroidal shell segments with thickness variation, in particular, have attracted the attention of many authors. Based on classical shell theory, Stein and McElman [39] studied the buckling of isotropic toroidal shell segments under mechanical loads. Oyesanya [40] utilized an analytical approach to investigate the buckling of initial imperfection toroidal shell segments based on Donnell shell theory. Weingarten et al. [41] presented an investigation on finite element shell-buckling of thin isotropic toroidal shell segments using classical thin shell theory. Recently, there has

been some research on buckling and post-buckling of the FGM toroidal shell segment. Ninh and Bich [42] investigated nonlinear vibration of simply supported FGM toroidal shell segment under mechanical load based on classical thin shell theory. Based on Reddy’s third-order shear deformation shell theory, Duc and Vuong [43] investigated the vibration behaviour of simply supported FGM toroidal shell segment with constant thickness under mechanical load. Long and Tung [44] studied buckling of FGM toroidal shell segment making use of Reddy’s higher order shear deformation shell theory. Thinh et al. [45] utilized the Galerkin method and the improved Donnell shell theory to investigate nonlinear buckling and postbuckling of FGM toroidal shell segments with thickness variation. In the above studies on isotropic and FGM toroidal shell segments, except for Thinh et al. [45], the main attention is focused on toroidal shell segments with constant thickness. Thinh et al. [45] utilized improved Donnell shell theory usually used for thin shells.

To the best of our knowledge, there are very rare studies focused on the variable thickness shell, and no works focused on the vibration of the thicker variable thickness FGM toroidal shell segment. Toroidal shell segment has been applied in practical fields such as oxygen tanks, rocket fuel tanks, underwater toroidal pressure hull, and satellite support structures. These structures may be made of FGM and have variable thickness. The study of vibration of variable thickness functionally graded toroidal shell segments is necessary and has practical significance. Thus, in this paper, for the first time, the nonlinear vibration response of toroidal shell segments with varying thickness subjected to external pressure is studied. The governing equations are derived based on Reddy’s third-order shear deformation shell theory with von Kármán nonlinearity. Galerkin method and Runge–Kutta method are used to solve the governing equations, and then the nonlinear vibration response of variable thickness FGM toroidal shell segment is analyzed.

## 2 Governing equations

A configuration of FGM toroidal shell segments of variable thickness  $h(x)$  and length  $L$  used in the present study is depicted in Fig. 1. The middle surface of the shell is formed by rotation of a plane circular arc of radius  $a$  about an axis in the plane of the curve. If  $a$  is positive, the shell is convex. If  $a$  is negative, the shell is concave. If  $a \rightarrow \infty$ , the toroidal shell segment becomes a cylindrical shell. The  $x$  coordinate of the shell is taken along the longitudinal direction,  $y$  coordinate along the circumferential direction and  $z$  along the thickness direction.

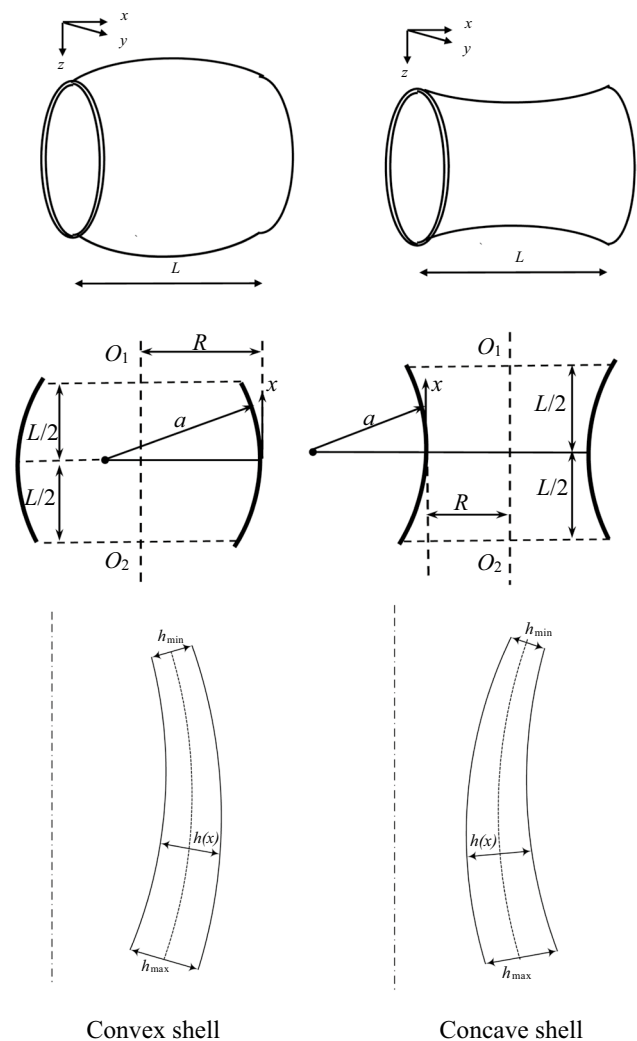


**Fig. 1** Geometry and coordinate system of variable thickness toroidal shell segments

Suppose that the inner surface of the FGM shell is ceramic-rich and the outer surface is metal-rich, and the material composition of the shell varies smoothly along the thickness direction according to a simple power-law in terms of the volume fractions of the constituents as Ninh and Bich [42]

$$E(x, z) = E_m + (E_c - E_m) \left( \frac{2z + h(x)}{2h(x)} \right)^k \tag{1}$$

$$\rho(x, z) = \rho_m + (\rho_c - \rho_m) \left( \frac{2z + h(x)}{2h(x)} \right)^k, \tag{2}$$

where  $m$  and  $c$  denote metal and ceramic, respectively.  $E_m, \rho_m, E_c, \rho_c$  are Young modulus and mass density of metal

and ceramic constituents, respectively.  $E(x, z)$  and  $\rho(x, z)$  indicate the effective properties of FGM. The non-negative number  $k$  is the volume fraction index defining the distribution of material constituents in FGM. The Poisson’s ratio of material constituents is assumed to be equal and to be constant, i.e.  $\nu_c = \nu_m = \text{const}$  Ninh and Bich [42].

In the present study, Reddy’s third-order shear deformation shell theory developed by Reddy and Liu [46] is used to investigate the nonlinear vibration of variable thickness FGM toroidal shell segments subjected to mechanical loads. According to this theory, the displacement components  $(u, v, w)$  can be written as

$$\begin{aligned} u(x, y, z, t) &= u_0(x, y, t) \left(1 - \frac{z}{a}\right) + \left[z - z^3 \frac{4}{3(h(x))^2}\right] \phi_x(x, y, t) - z^3 \frac{4}{3(h(x))^2} \frac{\partial w_0}{\partial x} \\ v(x, y, z, t) &= v_0(x, y, t) \left(1 - \frac{z}{R}\right) + \left[z - z^3 \frac{4}{3(h(x))^2}\right] \phi_y(x, y, t) - z^3 \frac{4}{3(h(x))^2} \frac{\partial w_0}{\partial y} \\ w(x, y, z, t) &= w_0(x, y, t), \end{aligned} \tag{3}$$

Substituting Eq. (3) into Eq. (4) and ignoring higher order terms on the assumption that  $1 - \frac{z}{a} \approx 1, 1 - \frac{z}{R} \approx 1$  leads to strain–displacement relations as:

$$\begin{aligned} \begin{pmatrix} \varepsilon_x \\ \varepsilon_y \\ \gamma_{xy} \end{pmatrix} &= \begin{pmatrix} \varepsilon_x^0 \\ \varepsilon_y^0 \\ \gamma_{xy}^0 \end{pmatrix} + z \begin{pmatrix} k_x^{(1)} \\ k_y^{(1)} \\ k_{xy}^{(1)} \end{pmatrix} + z^3 \begin{pmatrix} k_x^{(3)} \\ k_y^{(3)} \\ k_{xy}^{(3)} \end{pmatrix} + \frac{8z^3 \frac{\partial h(x)}{\partial x}}{3(h(x))^3} \begin{pmatrix} \phi_x + \frac{\partial w_0}{\partial x} \\ 0 \\ \phi_y + \frac{\partial w_0}{\partial y} \end{pmatrix}, \\ \begin{pmatrix} \gamma_{xz} \\ \gamma_{yz} \end{pmatrix} &= \begin{pmatrix} \gamma_{xz}^0 \\ \gamma_{yz}^0 \end{pmatrix} + z^2 \begin{pmatrix} k_{xz}^{(2)} \\ k_{yz}^{(2)} \end{pmatrix}, \end{aligned} \tag{5}$$

where

$$\begin{aligned} \begin{pmatrix} \varepsilon_x^0 \\ \varepsilon_y^0 \\ \gamma_{xy}^0 \end{pmatrix} &= \begin{pmatrix} \frac{\partial u_0}{\partial x} - \frac{w_0}{a} + \frac{1}{2} \left(\frac{\partial w_0}{\partial x}\right)^2 \\ \frac{\partial v_0}{\partial y} - \frac{w_0}{R} + \frac{1}{2} \left(\frac{\partial w_0}{\partial y}\right)^2 \\ \frac{\partial u_0}{\partial y} + \frac{\partial v_0}{\partial x} + \frac{\partial w_0}{\partial x} \frac{\partial w_0}{\partial y} \end{pmatrix}, \begin{pmatrix} k_x^{(1)} \\ k_y^{(1)} \\ k_{xy}^{(1)} \end{pmatrix} = \begin{pmatrix} \frac{\partial \phi_x}{\partial x} \\ \frac{\partial \phi_y}{\partial y} \\ \frac{\partial \phi_x}{\partial y} + \frac{\partial \phi_y}{\partial x} \end{pmatrix}, \begin{pmatrix} k_{xz}^{(2)} \\ k_{yz}^{(2)} \end{pmatrix} = -\frac{4}{(h(x))^2} \begin{pmatrix} \phi_x + \frac{\partial w_0}{\partial x} \\ \phi_y + \frac{\partial w_0}{\partial y} \end{pmatrix} \\ \begin{pmatrix} k_x^{(3)} \\ k_y^{(3)} \\ k_{xy}^{(3)} \end{pmatrix} &= -\frac{4}{3(h(x))^2} \begin{pmatrix} \frac{\partial \phi_x}{\partial x} + \frac{\partial^2 w_0}{\partial x^2} \\ \frac{\partial \phi_y}{\partial y} + \frac{\partial^2 w_0}{\partial y^2} \\ \frac{\partial \phi_x}{\partial y} + \frac{\partial \phi_y}{\partial x} + 2 \frac{\partial^2 w_0}{\partial x \partial y} \end{pmatrix}, \begin{pmatrix} \gamma_{xz}^0 \\ \gamma_{yz}^0 \end{pmatrix} = \begin{pmatrix} \phi_x + \frac{\partial w_0}{\partial x} \\ \phi_y + \frac{\partial w_0}{\partial y} \end{pmatrix}. \end{aligned} \tag{6}$$

where  $t$  is time,  $(u_0, v_0, w_0)$  are displacements of a point on the mid-surface, and  $\phi_x, \phi_y$  are the rotations of normal to the middle surface with respect to  $y$ - and  $x$ -axes, respectively.  $R$  is radius of equator.

Based on Reddy’s third-order shear deformation shell theory taking von Kármán nonlinearity into consideration, the normal strains  $(\varepsilon_x, \varepsilon_y)$ , in-plane shear strain  $(\gamma_{xy})$ , and transverse shear strains  $(\gamma_{xz}, \gamma_{yz})$  are expressed as Reddy and Liu [46]

$$\begin{aligned} \varepsilon_x &= \frac{\partial u}{\partial x} - \frac{1}{a}w + \frac{1}{2} \left(\frac{\partial w}{\partial x}\right)^2, \varepsilon_y = \frac{\partial v}{\partial y} - \frac{1}{R}w + \frac{1}{2} \left(\frac{\partial w}{\partial y}\right)^2. \\ \gamma_{xy} &= \frac{\partial u}{\partial y} + \frac{\partial v}{\partial x} + \frac{\partial w}{\partial x} \frac{\partial w}{\partial y}, \gamma_{xz} = \frac{\partial w}{\partial x} + \frac{\partial u}{\partial z} + \frac{1}{a}u, \gamma_{yz} = \frac{\partial w}{\partial y} + \frac{\partial v}{\partial z} + \frac{1}{R}v. \end{aligned} \tag{4}$$

The strain–displacement relations taking von Kármán nonlinearity for variable thickness shell presented in Eq. (5) is a novelty of the present study.

The stress–strain relations for variable thickness FGM toroidal shell segments using Hooke’s law are

$$\begin{aligned} \sigma_x &= \frac{E(x, z)}{1 - \nu^2} (\varepsilon_x + \nu \varepsilon_y), \sigma_y = \frac{E(x, z)}{1 - \nu^2} (\varepsilon_y + \nu \varepsilon_x) \\ \sigma_{xy} &= \frac{E(x, z)}{2(1 + \nu)} \gamma_{xy}, \sigma_{xz} = \frac{E(x, z)}{2(1 + \nu)} \gamma_{xz}, \sigma_{yz} = \frac{E(x, z)}{2(1 + \nu)} \gamma_{yz} \end{aligned} \tag{7}$$

where  $\nu$  is Poisson’s ratio,  $(\sigma_x, \sigma_y)$  are normal stresses,  $\sigma_{xy}$  is in-plane shear stress,  $(\sigma_{xz}, \sigma_{yz})$  are transverse shear stresses.

The force and moment resultants of variable thickness FGM toroidal shell segment are defined as

$$\begin{aligned}
 (N_i, M_i, P_i) &= \int_{-h(x)/2}^{h(x)/2} \sigma_i(1, z, z^3) dz, \quad (i = x; y; xy) \\
 (Q_j, R_j) &= \int_{-h(x)/2}^{h(x)/2} \sigma_{jz}(1, z^2) dz, \quad (j = x; y)
 \end{aligned}
 \tag{8}$$

Setting Eq. (1), Eq. (5), and Eq. (6) into Eq. (7) and then putting the results into Eq. (8) yields

$$\begin{aligned}
 \begin{pmatrix} N_x & N_y & N_{xy} \\ M_x & M_y & M_{xy} \\ P_x & P_y & P_{xy} \end{pmatrix} &= \begin{pmatrix} \Phi_{11} \left( \phi_x + \frac{\partial w_0}{\partial x} \right) & \Phi_{12} \left( \phi_x + \frac{\partial w_0}{\partial x} \right) & \Phi_{13} \left( \phi_y + \frac{\partial w_0}{\partial y} \right) \\ \Phi_{21} \left( \phi_x + \frac{\partial w_0}{\partial x} \right) & \Phi_{22} \left( \phi_x + \frac{\partial w_0}{\partial x} \right) & \Phi_{23} \left( \phi_y + \frac{\partial w_0}{\partial y} \right) \\ \Phi_{31} \left( \phi_x + \frac{\partial w_0}{\partial x} \right) & \Phi_{32} \left( \phi_x + \frac{\partial w_0}{\partial x} \right) & \Phi_{33} \left( \phi_y + \frac{\partial w_0}{\partial y} \right) \end{pmatrix} \\
 + \begin{pmatrix} Q_{11} & Q_{12} & Q_{13} \\ Q_{21} & Q_{22} & Q_{23} \\ Q_{31} & Q_{32} & Q_{33} \end{pmatrix} &\begin{pmatrix} \epsilon_x^0 + \nu \epsilon_y^0 & \epsilon_y^0 + \nu \epsilon_x^0 & 0.5(1-\nu) \gamma_{xy}^0 \\ k_x^{(1)} + \nu k_y^{(1)} & k_y^{(1)} + \nu k_x^{(1)} & 0.5(1-\nu) k_{xy}^{(1)} \\ k_x^{(3)} + \nu k_y^{(3)} & k_y^{(3)} + \nu k_x^{(3)} & 0.5(1-\nu) k_{xy}^{(3)} \end{pmatrix}
 \end{aligned}
 \tag{9}$$

$$\begin{pmatrix} Q_x & Q_y \\ R_x & R_y \end{pmatrix} = \begin{pmatrix} Q_{41} & Q_{42} \\ Q_{51} & Q_{52} \end{pmatrix} \begin{pmatrix} \gamma_{xz}^0 & \gamma_{yz}^0 \\ k_{xz}^{(2)} & k_{yz}^{(2)} \end{pmatrix},
 \tag{10}$$

where coefficients  $\Phi_{ij}(i = 1 - 3; j = 1 - 3)$ ,  $Q_{ij}(i = 1 - 3; j = 1 - 3)$ ,  $Q_{41}, Q_{42}, Q_{51}, Q_{52}$  are determined in Appendix A.

The equations of motion of the toroidal shell segment subjected to uniformly distributed external pressure  $q$  (N/m<sup>2</sup>) are given by Reddy and Liu [46]

$$\frac{\partial N_x}{\partial x} + \frac{\partial N_{xy}}{\partial y} = \bar{I}_1 \ddot{u}_0 + \bar{I}_2 \ddot{\phi}_x - \bar{I}_3 \frac{\partial \ddot{w}_0}{\partial x}
 \tag{11}$$

$$\frac{\partial N_{xy}}{\partial x} + \frac{\partial N_y}{\partial y} = \bar{I}'_1 \ddot{v}_0 + \bar{I}'_2 \ddot{\phi}_y - \bar{I}'_3 \frac{\partial \ddot{w}_0}{\partial y}
 \tag{12}$$

$$\begin{aligned}
 &\frac{\partial Q_x}{\partial x} + \frac{\partial Q_y}{\partial y} - \frac{4}{(h(x))^2} \left( \frac{\partial R_x}{\partial x} + \frac{\partial R_y}{\partial y} \right) + \frac{4}{3(h(x))^2} \left( \frac{\partial^2 P_x}{\partial x^2} + 2 \frac{\partial^2 P_{xy}}{\partial x \partial y} + \frac{\partial^2 P_y}{\partial y^2} \right) \\
 &+ \frac{1}{R} N_y + \frac{1}{a} N_x + N_x \frac{\partial^2 w_0}{\partial x^2} + 2 N_{xy} \frac{\partial^2 w_0}{\partial x \partial y} + N_y \frac{\partial^2 w_0}{\partial y^2} + q \\
 &= \bar{I}_1 \ddot{w}_0 + \bar{I}_3 \frac{\partial \ddot{u}_0}{\partial x} + \bar{I}_5 \frac{\partial \ddot{\phi}_x}{\partial x} + \bar{I}'_3 \frac{\partial \ddot{v}_0}{\partial y} + \bar{I}'_5 \frac{\partial \ddot{\phi}_y}{\partial y} - \frac{16}{9(h(x))^4} I_7 \left( \frac{\partial^2 \ddot{w}_0}{\partial x^2} + \frac{\partial^2 \ddot{w}_0}{\partial y^2} \right)
 \end{aligned}
 \tag{13}$$

$$\begin{aligned}
 &\frac{\partial M_x}{\partial x} + \frac{\partial M_{xy}}{\partial y} - Q_x + \frac{4}{(h(x))^2} R_x \\
 &- \frac{4}{3(h(x))^2} \left( \frac{\partial P_x}{\partial x} + \frac{\partial P_{xy}}{\partial y} \right) \\
 &= \bar{I}_2 \ddot{u}_0 + \bar{I}_4 \ddot{\phi}_x - \bar{I}_5 \frac{\partial \ddot{w}_0}{\partial x}
 \end{aligned}
 \tag{14}$$

$$\begin{aligned}
 &\frac{\partial M_y}{\partial y} + \frac{\partial M_{xy}}{\partial x} - Q_y + \frac{4}{(h(x))^2} R_y - \frac{4}{3(h(x))^2} \left( \frac{\partial P_y}{\partial y} + \frac{\partial P_{xy}}{\partial x} \right) \\
 &= \bar{I}'_2 \ddot{v}_0 + \bar{I}'_4 \ddot{\phi}_y - \bar{I}'_5 \frac{\partial \ddot{w}_0}{\partial y}
 \end{aligned}
 \tag{15}$$

The coefficients  $I_i, \hat{I}_i$  and  $\hat{I}'_i$  are determined in Appendix B. Substituting Eq. (9) and Eq. (10) into Eqs. (11) to (15) with the aid of Eq. (6) yields

$$\begin{aligned}
 &H_{11}(u_0) + H_{12}(v_0) + H_{13}(w_0) + H_{14}(\phi_x) + H_{15}(\phi_y) \\
 &= \bar{I}_1 \ddot{u}_0 + \bar{I}_2 \ddot{\phi}_x - \bar{I}_3 \frac{\partial \ddot{w}_0}{\partial x}
 \end{aligned}
 \tag{16}$$

$$\begin{aligned}
 &H_{21}(u_0) + H_{22}(v_0) + H_{23}(w_0) + H_{24}(\phi_x) + H_{25}(\phi_y) \\
 &= \bar{I}'_1 \ddot{v}_0 + \bar{I}'_2 \ddot{\phi}_y - \bar{I}'_3 \frac{\partial \ddot{w}_0}{\partial y}
 \end{aligned}
 \tag{17}$$

$$\begin{aligned}
 &H_{31}(u_0) + H_{32}(v_0) + H_{33}(w_0) + H_{34}(\phi_x) + H_{35}(\phi_y) + H_{36}(u_0, w_0) \\
 &+ H_{37}(v_0, w_0) + H_{38}(\phi_x, w_0) + H_{39}(\phi_y, w_0) + q = \bar{I}_1 \ddot{w}_0 + \bar{I}_3 \frac{\partial \ddot{u}_0}{\partial x} \\
 &+ \bar{I}'_3 \frac{\partial \ddot{v}_0}{\partial y} + \bar{I}_5 \frac{\partial \ddot{\phi}_x}{\partial x} + \bar{I}'_5 \frac{\partial \ddot{\phi}_y}{\partial y} - \frac{16}{9(h(x))^4} I_7 \left( \frac{\partial^2 \ddot{w}_0}{\partial x^2} + \frac{\partial^2 \ddot{w}_0}{\partial y^2} \right)
 \end{aligned}
 \tag{18}$$

$$\begin{aligned}
 &H_{41}(u_0) + H_{42}(v_0) + H_{43}(w_0) + H_{44}(\phi_x) + H_{45}(\phi_y) \\
 &= \bar{I}_2 \ddot{u}_0 + \bar{I}_4 \ddot{\phi}_x - \bar{I}_5 \frac{\partial \ddot{w}_0}{\partial x}
 \end{aligned}
 \tag{19}$$

$$\begin{aligned}
 &H_{51}(u_0) + H_{52}(v_0) + H_{53}(w_0) + H_{54}(\phi_x) + H_{55}(\phi_y) \\
 &= \bar{I}'_2 \ddot{v}_0 + \bar{I}'_4 \ddot{\phi}_y - \bar{I}'_5 \frac{\partial \ddot{w}_0}{\partial y}
 \end{aligned}
 \tag{20}$$

in which operators  $H_{1i}, H_{2i}, H_{4i}, H_{5i}(i = 1 - 5)$ ;  $H_{3i}(i = 1 - 9)$  are defined in Appendix C.

Equations (16) to (20) are five governing equations in terms of five variables  $u_0(x, y, t)$ ,  $v_0(x, y, t)$ ,  $w_0(x, y, t)$ ,  $\phi_x(x, y, t)$ , and  $\phi_y(x, y, t)$ . They are used to study the nonlinear vibration of variable thickness FGM toroidal shell segments based on Reddy's third-order shear deformation shell theory.

### 3 Galerkin procedure

In this study, variable thickness FGM toroidal shell segments are assumed to be simply supported at two butt-ends and subjected to external harmonic excitation. Thus, the associated boundary condition is

$$w_0 = 0, v_0 = 0, \phi_y = 0, M_x = 0, P_x = 0, N_{xy} = 0, N_x = 0 \text{ at } x = 0 \text{ and } x = L \tag{21}$$

The approximate solutions are chosen as

$$\begin{aligned} u_0(x, y, t) &= U(t) \cos \frac{m\pi x}{L} \sin \frac{ny}{R} \\ v_0(x, y, t) &= V(t) \sin \frac{m\pi x}{L} \cos \frac{ny}{R} \\ w_0(x, y, t) &= W(t) \sin \frac{m\pi x}{L} \sin \frac{ny}{R} \\ \phi_x(x, y, t) &= \Phi_x(t) \cos \frac{m\pi x}{L} \sin \frac{ny}{R} \\ \phi_y(x, y, t) &= \Phi_y(t) \sin \frac{m\pi x}{L} \cos \frac{ny}{R} \end{aligned} \tag{22}$$

where  $U(t), V(t), W(t), \Phi_x(t), \Phi_y(t)$  are unknown time-dependent functions,  $m$  and  $n$  are the numbers of half-waves in  $x$  and  $y$  directions, respectively. The boundary conditions  $w_0 = 0, v_0 = 0$ , and  $\phi_y = 0$  are satisfied at  $x = 0$  and  $x = L$ . The boundary conditions  $M_x = 0, P_x = 0, N_{xy} = 0, N_x = 0$  at  $x = 0$  and  $x = L$  are satisfied in average sense  $\frac{1}{2\pi R} \int_0^{2\pi R} M_x dy = 0, \frac{1}{2\pi R} \int_0^{2\pi R} P_x dy = 0, \frac{1}{2\pi R} \int_0^{2\pi R} N_x dy = 0$ , and  $\frac{1}{2\pi R} \int_0^{2\pi R} N_{xy} dy = 0$  at  $x = 0$  and  $x = L$ .

Substituting Eq. (22) into Eqs. (16) to (20) then applying the Galerkin method leads to

$$l_{11}U + l_{12}V + l_{13}W + l_{14}\Phi_x + l_{15}\Phi_y + l_{16}W^2 = l_{17}\ddot{U} + l_{18}\ddot{\Phi}_x + l_{19}\ddot{W} \tag{23}$$

$$l_{21}U + l_{22}V + l_{23}W + l_{24}\Phi_x + l_{25}\Phi_y + l_{26}W^2 = l_{27}\ddot{V} + l_{28}\ddot{\Phi}_y + l_{29}\ddot{W} \tag{24}$$

$$\begin{aligned} &l_{31}U + l_{32}V + l_{33}W + l_{34}\Phi_x + l_{35}\Phi_y \\ &+ l_{36}W^2 + l_{37}UW + l_{38}VW + l_{39}\Phi_x W + l_{310}\Phi_y W \\ &+ l_{311}W^3 + l_{312}q = l_{313}\ddot{U} + l_{314}\ddot{V} \\ &+ l_{315}\ddot{\Phi}_x + l_{316}\ddot{\Phi}_y + l_{317}\ddot{W} \end{aligned} \tag{25}$$

$$l_{41}U + l_{42}V + l_{43}W + l_{44}\Phi_x + l_{45}\Phi_y + l_{46}W^2 = l_{47}\ddot{U} + l_{48}\ddot{\Phi}_x + l_{49}\ddot{W} \tag{26}$$

$$l_{51}U + l_{52}V + l_{53}W + l_{54}\Phi_x + l_{55}\Phi_y + l_{56}W^2 = l_{57}\ddot{V} + l_{58}\ddot{\Phi}_y + l_{59}\ddot{W}, \tag{27}$$

where coefficients  $l_{1i}, l_{2i}, l_{4i}, l_{5i} (i = 1 - 9); l_{3i} (i = 1 - 17)$  are demonstrated in Appendix D.

On the whole, transverse nonlinear vibration is a primary motion for the FGM variable thickness toroidal shell segments, thereby, we can suppose that the four right sides of the four Eqs. (23), (24), (26) and (27) to be equal to zero. With this assumption, the system of five Eqs. (23)–(27) can be converted into the following equation:

$$(1 + D_1 W)\ddot{W} + D_2 W + D_3 W^2 + D_4 W^3 + D_5 q = 0, \tag{28}$$

where coefficients  $D_i (i = 1 - 6)$  are determined in Appendix E.

#### 3.1 Natural frequency

The natural frequencies of FGM variable thickness toroidal shell segments with subscripts  $m$  and  $n$  are the mode shapes in the  $x$  and  $y$  directions, respectively, can be determined from Eq. (28) as

$$\omega_{mn} = \sqrt{D_2}. \tag{29}$$

#### 3.2 Nonlinear forced vibrations

Consider FGM variable thickness toroidal shell segments subjected to external harmonic excitation  $q = Q \sin \Omega t$ .  $Q$  and  $\Omega$  are assumed to be time independent. Substituting  $q = Q \sin \Omega t$  into Eq. (28) and using the Runge–Kutta method, the nonlinear forced vibration of variable thickness FGM toroidal shell segments is calculated and analyzed.

### 4 Numerical analysis

#### 4.1 Comparisons

This part shows three comparisons to verify the accuracy of the present approach. Firstly, consider an isotropic cylindrical shell with linear asymmetric variation thickness along the axial direction. Material parameters are taken as Sivadas and Ganesan [13]  $E = 2.035 \times 10^{11}$  Pa,  $\nu = 0.285$ ,  $\rho = 7846$  kg/m<sup>3</sup>. The average thickness, equator radius, and length of the shell is chosen as Sivadas and Ganesan [13]  $h_{av} = 0.508$  mm,  $R = 100h_{av}$ ,  $L = 0.5R$ , respectively. The thickness of the shell linearly varies from the value  $h_{min}$  to the value  $h_{max}$ . Thereby, the thickness is defined as  $h(x) = \frac{2h_{av}}{1+\beta} \left( \beta - \frac{\beta-1}{L}x \right)$ , in which  $\beta = \frac{h_{max}}{h_{min}}$ . Using Eq. (29) ( $a \rightarrow \infty$ ), the lowest natural frequencies (minimize the function  $\frac{\omega_{mn}}{2\pi}$  with respect to  $m$  and  $n$ ) are calculated and shown in



**Table 1** Comparison of lowest natural frequencies for material isotropic, linear symmetric variation cylindrical shell

$\beta = \frac{h_{\max}}{h_{\min}}$	Sivadas and Ganesan [13]	Present study	Errors (%)
1	7730.8	7765.6	0.45
2	8025.4	7930.3	1.19
3	8238.6	8111.8	1.54
4	8397.1	8228.0	2.01
5	8517.6	8316.0	2.36
6	8611.4	8383.9	2.64
7	8685.9	8437.5	2.86
8	8746.0	8480.7	3.03
9	8795.3	8516.2	3.17

Table 1 in comparison with the results given by Sivadas and Ganesan [13] using Love’s first approximation shell theory and semi-analytical finite element approach. As can be seen, a good agreement is obtained in this comparison.

Secondly, consider an FGM cylindrical shell with linear asymmetric variation thickness along the axial direction. The material parameters are chosen as Phu et al. [34]:  $E_m = 70 \text{ GPa}$ ,  $\rho_m = 2702 \text{ kg/m}^3$ ,  $E_c = 380 \text{ GPa}$ ,  $\rho_c = 3800 \text{ kg/m}^3$ ,  $\nu_m = \nu_c = 0.3$ . The thickness of FGM shell varies linearly along the axial direction from a value  $h_{\min} = 0.004 \text{ m}$  to a value  $h_{\max} = 0.006 \text{ m}$ . The radius and length of shell are chosen as  $R = 200h_{\min}$ ,  $L = 2R$ . The natural frequencies are calculated and compared with the results reported by Phu et al. [34] in Table 2 using classical thin shell theory and Galerikin method. Again, a good agreement is obtained.

Thirdly, an FGM toroidal shell segment is considered with material and geometrical parameters as Ninh and Bich [42]:  $E_m = 70 \times 10^9 \text{ Pa}$ ,  $\rho_m = 2702 \text{ kg/m}^3$ ,  $E_c = 380 \times 10^9 \text{ Pa}$ ,  $\rho_c = 3800 \text{ kg/m}^3$ ,  $\nu_m = \nu_c = 0.3$ ,  $h = 0.01 \text{ m}$ ,  $a/R = 10$ ,  $L/R = 0.5$ ,  $k = 5$ . The external harmonic excitation is chosen as  $q = 1000 \sin 6000t \text{ Pa}$ . The lowest natural frequencies are calculated by minimizing the function  $\frac{\omega_{mn}}{2\pi}$  with respect to  $m$  and  $n$  of the present study and compared with those calculated by Eq. (21) of Ninh and Bich [42]. The results are listed in Table 3. The vibration response is

**Table 2** Comparison of natural frequencies for variable thickness FGM cylindrical shell

$\omega_{mn}$	Phu et al. [34]	Present study	Errors (%)
$\omega_{11}$	4932.38	4933.41	0.021
$\omega_{13}$	1487.72	1494.45	0.45
$\omega_{15}$	641.99	659.59	2.74
$\omega_{17}$	502.50	524.81	4.40
$\omega_{19}$	676.96	688.78	1.75

**Table 3** Comparison of the lowest natural frequencies for FGM toroidal shell segment

	Ninh and Bich [42]	Present study	Errors (%)
Convex shell $a/R = 10$			
$R/h = 30$	20056.04	19927.49	0.64
$R/h = 40$	13196.48	13140.29	0.43
$R/h = 50$	9545.28	9524.68	0.22
$R/h = 100$	3512.21	3508.65	0.1
$R/h = 150$	1970.59	1969.72	0.05
Concave shell $a/R = -10$			
$R/h = 30$	18914.27	18778.26	0.72
$R/h = 40$	12159.17	12098.39	0.5
$R/h = 50$	8618.54	8595.85	0.26
$R/h = 100$	2925.33	2922.62	0.09
$R/h = 150$	1536.82	1535.71	0.07

compared on Fig. 2. Obviously, a good agreement is obtained in this comparison. Moreover, the lowest natural frequencies of FGM toroidal shell segment calculated in the present study using the Reddy’s third-order shear deformation shell theory ( $f^{TSDT}$ ) are smaller than corresponding values calculated by Eq. (21) of Ninh and Bich [42] using the classical thin shell theory ( $f^{CST}$ ). The error  $\left(\frac{f^{CST} - f^{TSDT}}{f^{CST}} \cdot 100\%\right)$  decreases as the  $R/h$  ratio increases. The information in Fig. 2 reveals that the difference between two amplitudes is  $\frac{4.0273e-8 - 3.837e-8}{4.0273e-8} \approx 4.7\%$ .

### 4.2 Nonlinear vibration analysis of FGM variable thickness toroidal shell segments

This section considers FGM variable thickness toroidal shell segments with the material properties are as  $E_m = 105.6960 \text{ GPa}$ ,  $E_c = 154.3211 \text{ GPa}$ ,  $\nu = 0.2980$ ,  $\rho_m = 4429 \text{ kg/m}^3$ ,  $\rho_c = 5700 \text{ kg/m}^3$ . The thickness of the shell is assumed to be linearly varied along the axial direction from the value  $h_{\min}$  to the value  $h_{\max}$ , and defined as  $h(x) = \frac{2h_{av}}{1+\beta} \left(\beta - \frac{\beta-1}{L}x\right)$ , in which  $h_{av}$  is average thickness, and  $\beta = \frac{h_{\max}}{h_{\min}}$  is variation parameter. Using the Runge–Kutta method to solve Eq. (28), the effects of variation parameter, volume fraction index, and geometrical parameters on natural frequencies and nonlinear vibration response are investigated.

#### 4.2.1 Natural frequencies

Effect of variation parameter  $\beta$  on natural frequencies of FGM variable thickness toroidal shell segments is illustrated in Table 4. Parameters are chosen as  $h_{av} = 0.02 \text{ m}$ ,

**Fig. 2** Comparison of forced vibration response of FGM toroidal shell segment

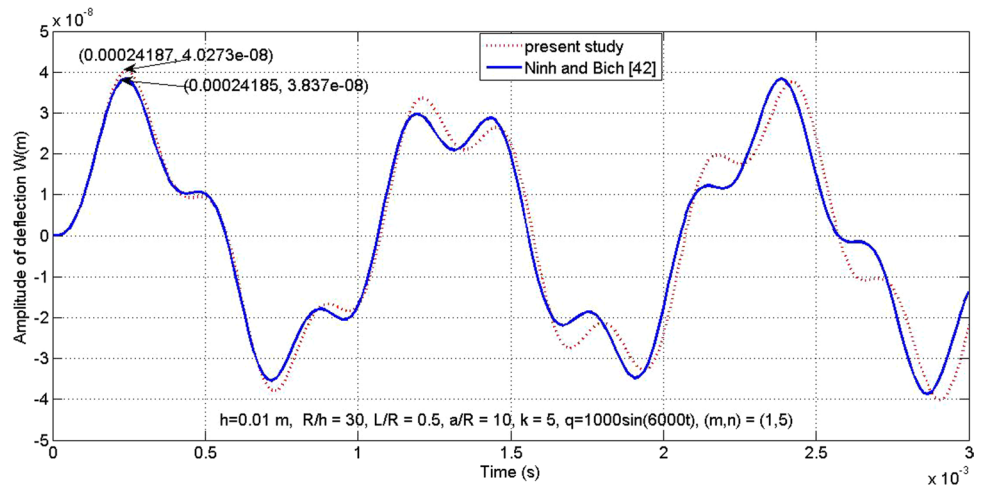


**Table 4** Natural frequencies of FGM toroidal shell segment with different variation parameter ( $h_{av} = 0.02$  m,  $R/h_{av} = 100$ ,  $L/R = 1$ ,  $a/R = 10$ ,  $k = 2$ )

$m$	$n$	$\frac{\omega_{mn}}{2\pi}$ (Hz)				
		$\beta = 1$	$\beta = 2$	$\beta = 3$	$\beta = 4$	$\beta = 5$
1	1	357.0417	357.0847	357.1192	357.1440	357.1624
	2	284.8968	284.9592	285.0359	285.0964	285.1429
	3	221.0859	221.2078	221.3722	221.5038	221.6053
	4	174.9403	175.1940	175.5312	175.8003	176.0074
	5	144.8768	145.3776	146.0255	146.5395	146.9337
	6	127.9007	128.7968	129.9324	130.8276	131.5113
	7	121.7341	123.1673	124.9569	126.3583	127.4241
	8	124.5932	126.6545	129.2017	131.1850	132.6874
	9	134.8084	137.5327	140.8762	143.4689	145.4273
	10	150.8745	154.2690	158.4178	161.6269	164.0467
2	1	391.8222	392.2042	392.5788	392.8620	393.0751
	2	367.5272	367.9571	368.4167	368.7702	369.0382
	3	334.7282	335.2694	335.9008	336.3942	336.7705
	4	300.2056	300.9630	301.8973	302.6335	303.1968
	5	268.8250	269.9558	271.3830	272.5098	273.3720
	6	243.4554	245.1728	247.3463	249.0584	250.3657
	7	225.5763	228.1369	231.3562	233.8795	235.7992
	8	215.7957	219.4642	224.0298	227.5855	230.2781
	9	214.1014	219.1041	225.2641	230.0285	233.6193
	10	219.9879	226.4825	234.4032	240.4909	245.0592

$R/h_{av} = 100$ ,  $L/R = 1$ ,  $a/R = 10$ ,  $k = 2$ . It can be seen that with the same mode numbers, the shell with a constant thickness corresponding to  $\beta = \frac{h_{max}}{h_{min}} = 1$  has the lowest frequency in comparison with variable thickness shells. In addition, the natural frequency slightly increases as the variation parameter increases. For example, as variation parameter increases from value  $\beta = 1$  to the value  $\beta = 5$ , the natural frequency increases by 1.4%, 2.8%, 4.7%, 6.5%, 7.9%, and 8.7% corresponding to mode numbers  $(m, n) = (1, 5)$ ,  $(1, 6)$ ,  $(1, 7)$ ,  $(1, 8)$ ,  $(1, 9)$ , and  $(1, 10)$ , respectively.

Effects of the volume fraction index and  $L/R$  ratio on natural frequencies of FGM variable thickness toroidal shell segments are shown in Table 5. Parameters are taken as  $h_{av} = 0.02$  m,  $R = 100h_{av}$ ,  $a = 10R$ ,  $\beta = 2$ ,  $k = 1$ ,  $(m, n) = (1, 1)$ . It can be seen that for all cases of  $L/R$  ratio, there is a decreasing trend of natural frequencies as the volume fraction index  $k$  increases. This can be explained by the fact that as the volume fraction index  $k$  increases, the percentage of ceramic in FGM decreases, and the shell will be softer, leading to the decrease of natural frequency.



**Table 5** Natural frequencies of FGM toroidal shell segment with different volume fraction index and different  $L/R$  ratio ( $h_{av} = 0.02$  m,  $R = 100h_{av}$ ,  $a = 10R$ ,  $\beta = 2$ ,  $(m, n) = (1, 1)$ )

$k$	$\frac{\omega_{11}}{2\pi}$ (Hz)				
	$L/R = 0.5$	$L/R = 1$	$L/R = 1.5$	$L/R = 2$	$L/R = 3$
0	406.6032	370.6200	317.3324	260.8906	178.4305
0.1	404.9239	369.0486	315.9767	259.7704	177.6608
0.2	403.4597	367.6817	314.7984	258.7972	176.9925
0.5	400.0162	364.4743	312.0368	256.5182	175.4287
1	396.2358	360.9583	309.0147	254.0277	173.7218
5	387.3850	352.7886	302.0204	248.2813	169.7945
10	385.0004	350.6703	300.2185	246.8065	168.7899
$\infty$	381.7438	347.9606	297.9309	244.9400	167.5214

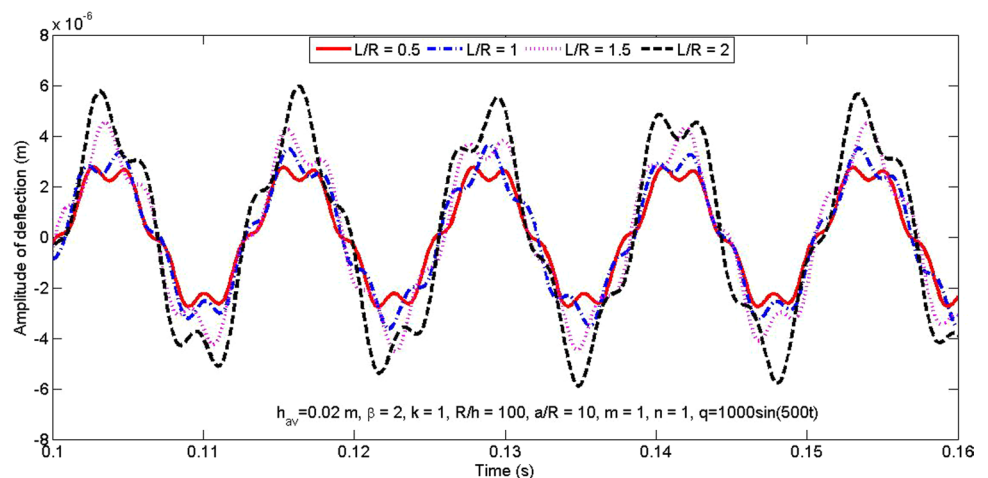
Numerical values in Table 5 also show that there is also a decreasing trend of natural frequencies as the  $L/R$  ratio increases. For example, as the  $L/R$  ratio increases from 0.5 to 1, the natural frequency decreases by 8.85%, 8.86%, and 8.87% corresponding to  $k = 0$ ,  $k = 0.1$ , and  $k = 0.2$ , respectively.

**Table 6** Natural frequencies of convex and concave shells with different  $a/L$  and  $L/R$  ratios ( $R = 2$  m,  $L = 2$  m,  $\beta = 2$ ,  $k = 1$ ,  $(m, n) = (1, 3)$ )

Type of shells	$a/L$	$\frac{\omega_{13}}{2\pi}$ (Hz)				
		$R/h_{av} = 50$	$R/h_{av} = 100$	$R/h_{av} = 150$	$R/h_{av} = 200$	$R/h_{av} = 500$
Convex shells	$\infty$	208.3914	204.5827	203.8635	203.6095	203.3311
	20	217.7473	214.0863	213.3938	213.1487	212.8786
	15	220.8669	217.2524	216.5683	216.3260	216.0584
	10	227.1057	223.5807	222.9126	222.6756	222.4130
	5	245.8012	242.5186	241.8938	241.6711	241.4215
Concave shells	-5	171.1461	166.5923	165.7359	165.4358	165.1132
	-10	189.7168	185.5709	184.7901	184.5155	184.2175
	-15	195.9334	191.9068	191.1479	190.8806	190.5897
	-20	199.0453	195.0756	194.3271	194.0633	193.7757

Table 6 depicts how the values of  $a/L$  and  $R/h_{av}$  ratios affect the natural frequency of FGM variable thickness toroidal shell segment. It is seen from the table that for all cases of convex shells and concave shells, there is a decreasing trend of natural frequencies as the  $R/h_{av}$  ratio increases. For example, in the case of convex shells and  $a/L = 5$ , as the  $R/h_{av}$  ratio increases from 50 to 100, 150, 200, and 500 the natural frequency of the shell decreases by 1.33%, 1.59%, 1.68%, and 1.78%, respectively. In the case of concave shells and  $a/L = -5$ , the natural frequency of the shell decreases by 2.66%, 3.16%, 3.34%, and 3.53%, respectively, as the  $R/h_{av}$  ratio increases from 50 to 100, 150, 200, and 500. The result in Table 6 also shows that in the case of convex shells, as the  $a/L$  ratio increases the natural frequency of FGM variable thickness toroidal shell segments decreases. However, there is a trend in the opposite direction for the case of the concave shell. The natural frequency of the concave shell decreases as the  $a/L$  ratio decreases. For example, in the case of convex shells and  $R/h_{av} = 50$ , the natural frequency decreases by 7.6%, 10.14%, 11.41%, and 15.22%, respectively, as the  $a/L$  ratio increases from 5 to 10, 15, 20, and  $\infty$ . In the case of concave shells and  $R/h_{av} = 50$ , as the  $a/L$  ratio increases from -5

**Fig. 3** The effect of  $L/R$  ratio on nonlinear vibration responses of FGM variable thickness toroidal shell segments with mode numbers  $(m, n) = (1, 1)$



to  $-10$ ,  $-15$ , and  $-20$  the natural frequency increases by 10.85%, 14.48%, and 16.3%, respectively. In addition, the natural frequencies of convex shells are greater than the ones of concave shells.

### 4.2.2 Nonlinear vibration responses

Figures 3, 4 and 5 depict the nonlinear vibration responses of FGM variable thickness toroidal shell segments corresponding to mode numbers  $(m, n) = (1, 1)$ ,  $(m, n) = (1, 3)$ ,

**Fig. 4** The effect of  $L/R$  ratio on nonlinear vibration responses of FGM variable thickness toroidal shell segments with mode numbers  $(m, n) = (1, 3)$

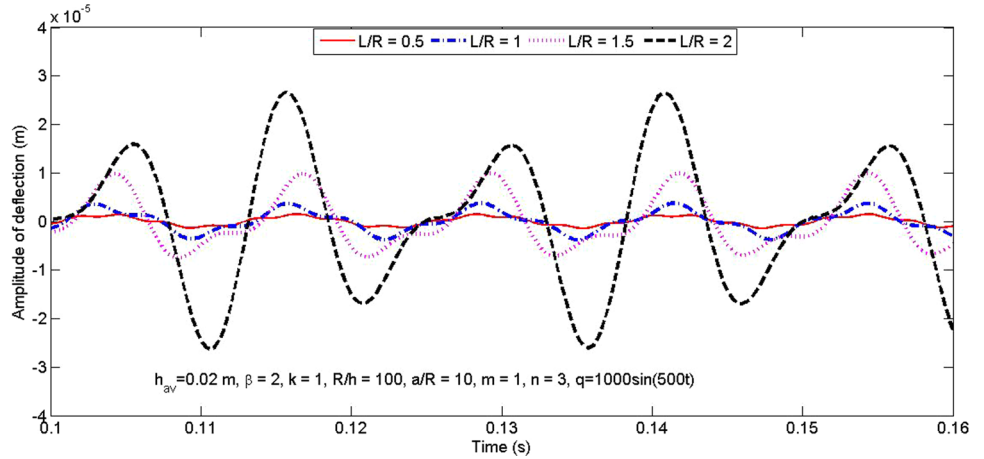


**Fig. 5** The effect of  $L/R$  ratio on nonlinear vibration responses of FGM variable thickness toroidal shell segments with mode numbers  $(m, n) = (3, 3)$

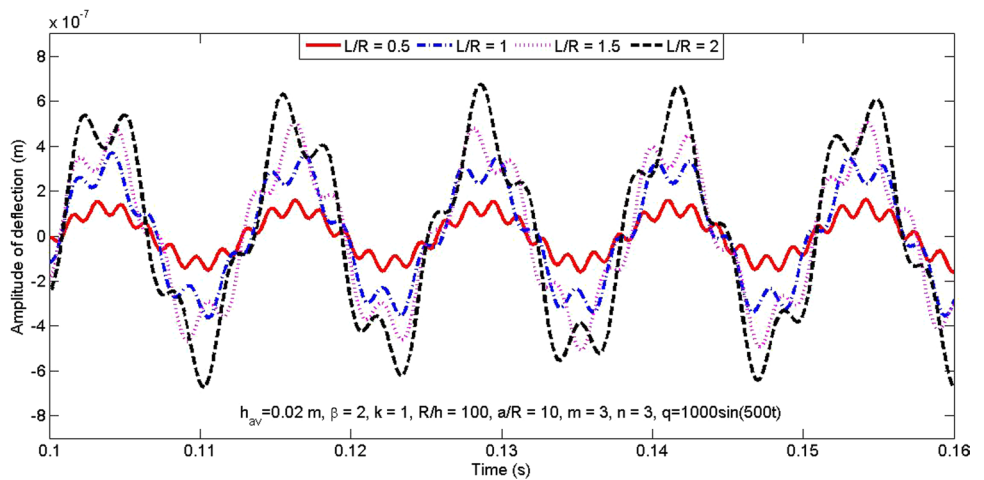


**Fig. 6** The effect of  $R/h_{av}$  ratio on nonlinear vibration responses of FGM variable thickness toroidal shell segments with mode numbers  $(m, n) = (1, 1)$

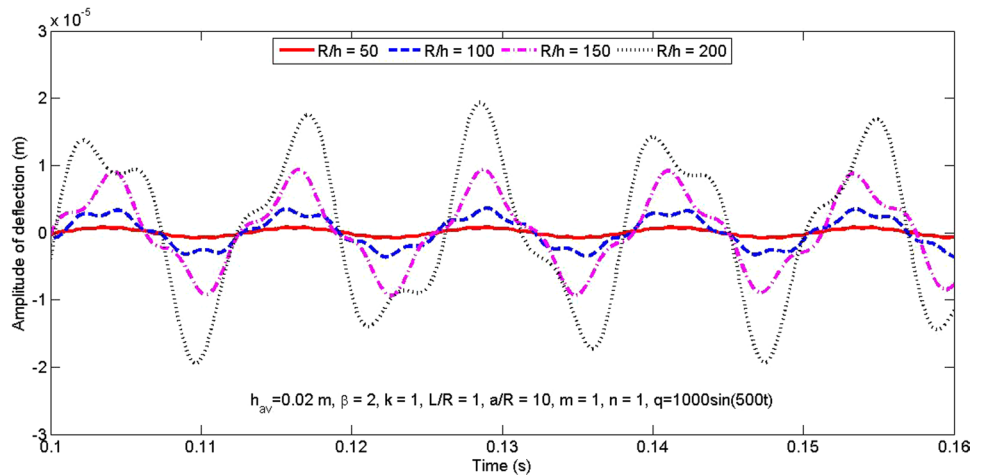


**Fig. 7** The effect of  $R/h_{av}$  ratio on nonlinear vibration responses of FGM variable thickness toroidal shell segments with mode numbers  $(m, n) = (1, 3)$

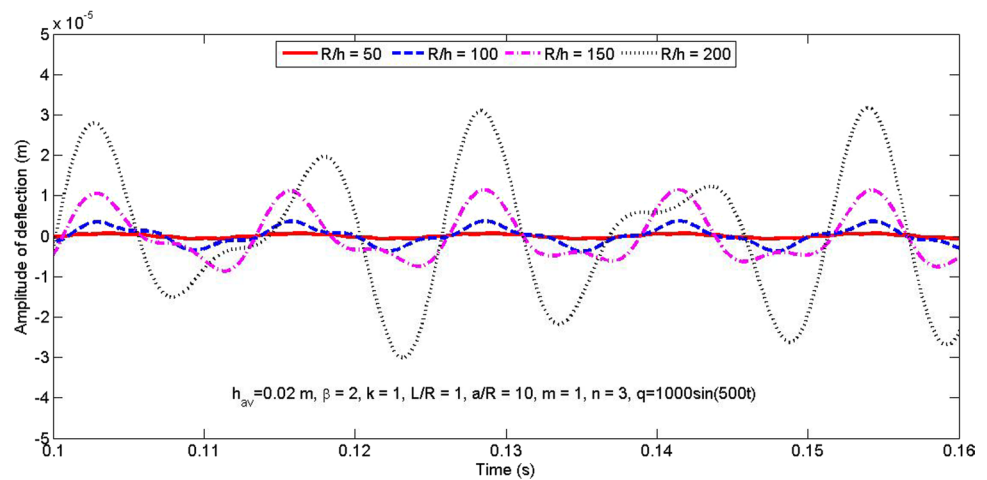
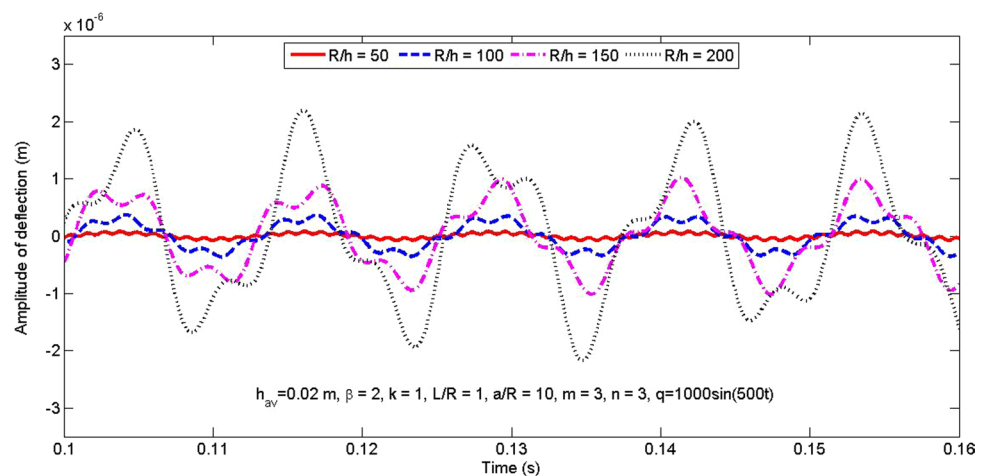


**Fig. 8** The effect of  $R/h_{av}$  ratio on nonlinear vibration responses of FGM variable thickness toroidal shell segments with mode numbers  $(m, n) = (3, 3)$



and  $(m, n) = (3, 3)$ , respectively. In each figure, four cases of  $L/R$  ratio ( $L/R = 0.5, 1, 1.5$  and  $2$ ) are considered. Other parameters are indicated in the figures. It can be seen from these figures that for all cases of mode numbers  $(m, n)$ , the vibration amplitude of FGM variable thickness toroidal shell segment increases as the  $L/R$  ratio increases. This indicates that a longer shell has greater vibration amplitude than that of a shorter one.

The effect of  $R/h_{av}$  ratio on vibration response of FGM variable thickness toroidal shell segment is illustrated in Figs. 6, 7 and 8 corresponding to mode numbers  $(m, n) = (1, 1)$ ,  $(m, n) = (1, 3)$ , and  $(m, n) = (3, 3)$ , respectively. Each figure draws four curves of vibration response corresponding to  $R/h_{av} = 50$ ,  $R/h_{av} = 100$ ,  $R/h_{av} = 150$ , and  $R/h_{av} = 200$ . Other parameters are indicated in each figure. The result in these figures shows that the vibration amplitude of FGM variable thickness toroidal shell segments decreases significantly as the  $R/h_{av}$  ratio decreases for all three cases of mode numbers. It means that the

vibration response of FGM variable thickness toroidal shell segment is very sensitive to the change of the  $R/h_{av}$  ratio.

The volume fraction index  $k$  is a parameter that defines the contribution of material constituents in FGM. It can be seen from Eq. (1) that as the volume fraction index  $k$  increase, the volume fraction of ceramic constituent decreases, and the volume fraction of metal constituent increases in FGM. Therefore, the volume fraction index  $k$  affects effective Young modulus and effective mass density of FGM, leading to the effect on vibration response of FGM variable thickness toroidal shell segment. This effect is illustrated in Figs. 9, 10, 11 and 12 corresponding to mode numbers  $(m, n) = (1, 1)$ ,  $(m, n) = (1, 3)$ ,  $(m, n) = (3, 1)$ , and  $(m, n) = (3, 3)$ , respectively. In each figure, three cases ( $k = 0.1$ ,  $k = 1$ , and  $k = 10$ ) are considered. It can be seen that the metal-rich shell ( $k = 10$ ) has a larger vibration amplitude in comparison with that of the other cases.

**Fig. 9** The effect of volume fraction index on nonlinear vibration responses of FGM variable thickness toroidal shell segments with mode numbers  $(m, n) = (1, 1)$

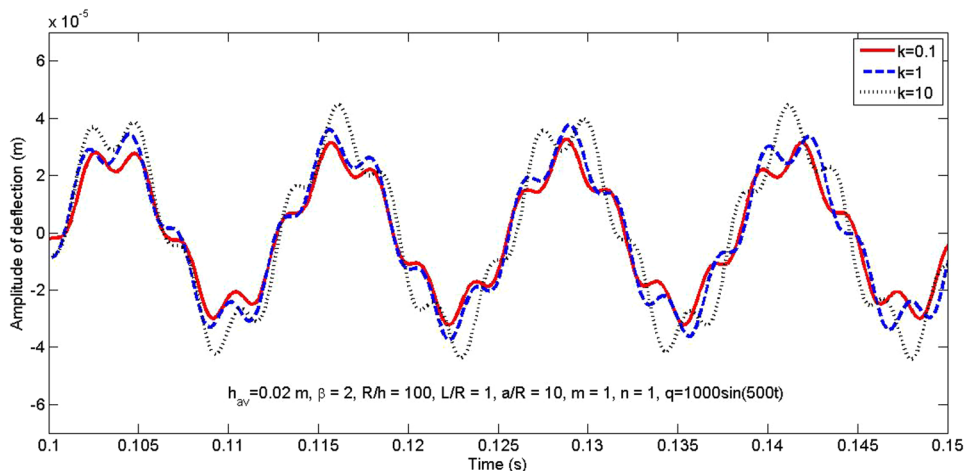


**Fig. 10** The effect of volume fraction index on nonlinear vibration responses of FGM variable thickness toroidal shell segments with mode numbers  $(m, n) = (1, 3)$

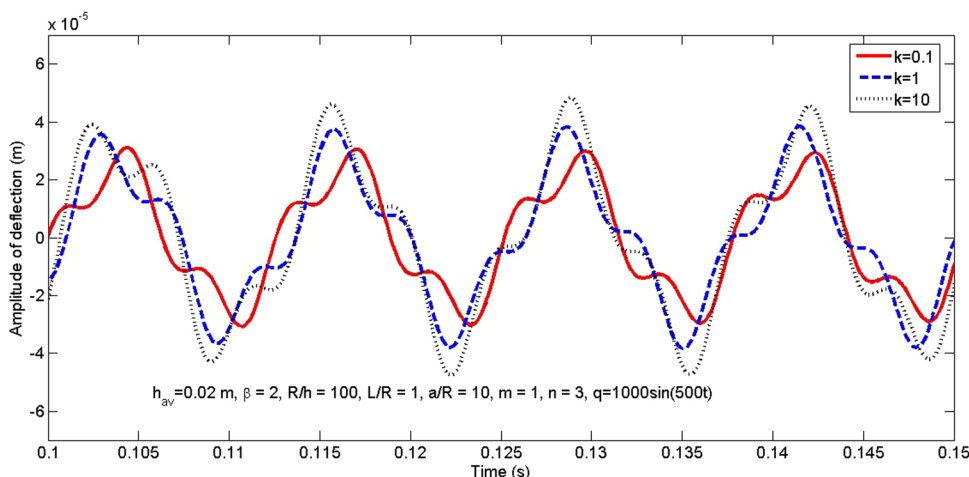
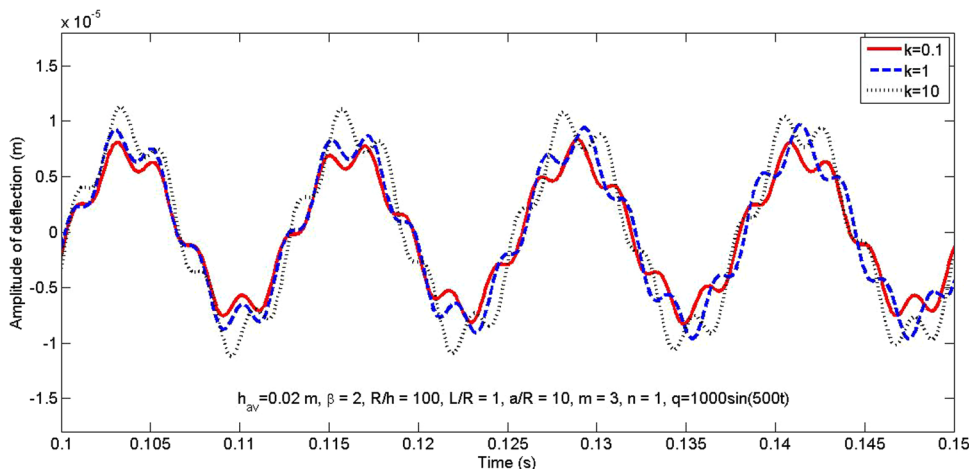


**Fig. 11** The effect of volume fraction index on nonlinear vibration responses of FGM variable thickness toroidal shell segments with mode numbers  $(m, n) = (3, 1)$

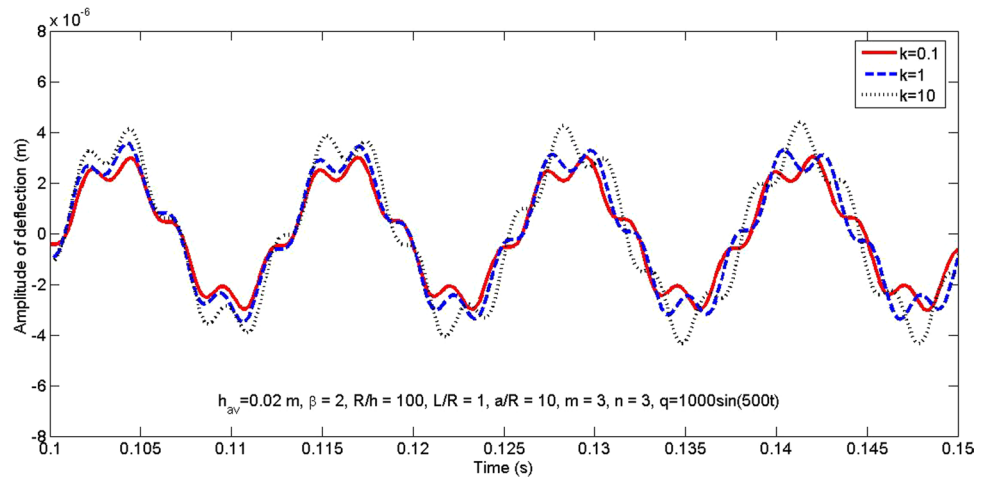


### 5 Conclusions

An analytical investigation of the vibration of the FGM variable thickness toroidal shell segment is presented in this

study. Firstly, based on Reddy’s third-order shear deformation shell theory, the governing partial differential equations of motion of FGM variable thickness toroidal shell segment are obtained. Secondly, the Galerkin method is used

**Fig. 12** The effect of volume fraction index on nonlinear vibration responses of FGM variable thickness toroidal shell segments with mode numbers  $(m, n) = (3, 3)$



to convert the system of partial differential equations into nonlinear differential equations. Lastly, the Runge–Kutta method is used to solve the nonlinear differential equation of motion, and then the vibration response is studied. The effects of geometric, material, and variation parameters on natural frequency and vibration response are analyzed and discussed. It is revealed that shell with a constant thickness has the lowest frequency in comparison with variable thickness shells. The natural frequency increases as the volume fraction index decreases. Geometrical parameters have significant effect on natural frequency and vibration response of variable thickness toroidal shell segment.

with

$$E_1 = E_m + \frac{E_{cm}}{k + 1}, E_2 = \frac{E_{cm}k}{2(k + 1)(k + 2)},$$

$$E_3 = \frac{E_m}{12} + E_{cm} \left[ \frac{1}{k + 3} - \frac{1}{k + 2} + \frac{1}{4(k + 1)} \right],$$

$$E_4 = E_{cm} \left[ \frac{1}{k + 4} - \frac{3}{2(k + 3)} + \frac{3}{4(k + 2)} - \frac{1}{8(k + 1)} \right],$$

### Appendix A

$$\Phi_{11} = \frac{8E_4}{3(1 - \nu^2)} h(x)h'(x), \Phi_{12} = \frac{8\nu E_4}{3(1 - \nu^2)} h(x)h'(x), \Phi_{13} = \frac{4E_4}{3(1 + \nu)} h(x)h'(x)$$

$$\Phi_{21} = \frac{8E_5}{3(1 - \nu^2)} (h(x))^2 h'(x), \Phi_{22} = \frac{8\nu E_5}{3(1 - \nu^2)} (h(x))^2 h'(x), \Phi_{23} = \frac{4E_5}{3(1 + \nu)} (h(x))^2 h'(x)$$

$$\Phi_{31} = \frac{8E_7}{3(1 - \nu^2)} (h(x))^4 h'(x), \Phi_{32} = \frac{8\nu E_7}{3(1 - \nu^2)} (h(x))^4 h'(x),$$

$$\Phi_{33} = \frac{4E_7}{3(1 + \nu)} (h(x))^4 h'(x), Q_{11} = \frac{E_1}{1 - \nu^2} h(x), Q_{12} = \frac{E_2}{1 - \nu^2} (h(x))^2, Q_{13} = \frac{E_4}{1 - \nu^2} (h(x))^4,$$

$$Q_{21} = \frac{E_2}{1 - \nu^2} (h(x))^2, Q_{22} = \frac{E_3}{1 - \nu^2} (h(x))^3, Q_{23} = \frac{E_5}{1 - \nu^2} (h(x))^5, Q_{31} = \frac{E_4}{1 - \nu^2} (h(x))^4,$$

$$Q_{32} = \frac{E_5}{1 - \nu^2} (h(x))^5, Q_{33} = \frac{E_7}{1 - \nu^2} (h(x))^7, Q_{41} = \frac{E_1}{2(1 + \nu)} h(x), Q_{42} = \frac{E_3}{2(1 + \nu)} (h(x))^3,$$

$$Q_{51} = \frac{E_3}{2(1 + \nu)} (h(x))^3, Q_{52} = \frac{E_5}{2(1 + \nu)} (h(x))^5,$$



$$E_5 = \frac{E_m}{80} + E_{cm} \left[ \frac{1}{k+5} - \frac{2}{k+4} + \frac{3}{2(k+3)} - \frac{1}{2(k+2)} + \frac{1}{16(k+1)} \right],$$

$$E_7 = \frac{E_m}{448} + E_{cm} \left[ \frac{1}{k+7} - \frac{3}{k+6} + \frac{15}{4(k+5)} - \frac{5}{2(k+4)} + \frac{15}{16(k+3)} - \frac{3}{16(k+2)} + \frac{1}{64(k+1)} \right].$$

$$\bar{I}_5 = \bar{I}'_5 = \left( \frac{4I_5}{3} - \frac{16}{9}I_7 \right) (h(x))^3,$$

$$I_i = \frac{1}{h'(x)} \cdot \int_{-h(x)/2}^{h(x)/2} \rho(z) z^{i-1} dz, \quad (i = 1, 2, 3, 4, 5, 7).$$

### Appendix C

$$H_{11}(u_0) = \frac{E_1}{1-\nu^2} \frac{\partial \left[ h(x) \frac{\partial u_0}{\partial x} \right]}{\partial x} + \frac{E_1}{2(1+\nu)} h(x) \frac{\partial^2 u_0}{\partial y^2}.$$

$$H_{12}(v_0) = \frac{E_1 \nu}{1-\nu^2} \frac{\partial \left[ h(x) \frac{\partial v_0}{\partial y} \right]}{\partial x} + \frac{E_1}{2(1+\nu)} h(x) \frac{\partial^2 v_0}{\partial x \partial y}.$$

$$H_{13}(w_0) = H_{13a}(w_0) + H_{13b}(w_0).$$

$$H_{13a}(w_0) = \frac{-E_1}{1-\nu^2} \left( \frac{1}{a} + \frac{\nu}{R} \right) \frac{\partial [h(x)w_0]}{\partial x} + \frac{2cE_4}{1-\nu^2} \frac{\partial \left[ h(x) \frac{\partial h(x)}{\partial x} \frac{\partial w_0}{\partial x} \right]}{\partial x} - \frac{cE_4}{1-\nu^2} \frac{\partial \left[ (h(x))^2 \left( \frac{\partial^2 w_0}{\partial x^2} + \nu \frac{\partial^2 w_0}{\partial y^2} \right) \right]}{\partial x} + \frac{cE_4}{1+\nu} h(x) \frac{\partial h(x)}{\partial x} \frac{\partial^2 w_0}{\partial y^2} - \frac{cE_4}{1+\nu} (h(x))^2 \frac{\partial^3 w_0}{\partial x \partial y^2}.$$

$$H_{13b}(w_0) = \frac{E_1}{2(1-\nu^2)} \frac{\partial \left[ h(x) \left( \left( \frac{\partial w_0}{\partial x} \right)^2 + \nu \left( \frac{\partial w_0}{\partial y} \right)^2 \right) \right]}{\partial x} + \frac{E_1 h(x)}{2(1+\nu)} \frac{\partial \left( \frac{\partial w_0}{\partial x} \frac{\partial w_0}{\partial y} \right)}{\partial y}.$$

$$H_{14}(\phi_x) = \frac{E_2 - cE_4}{1-\nu^2} \frac{\partial \left[ (h(x))^2 \frac{\partial \phi_x}{\partial x} \right]}{\partial x} + \frac{2cE_4}{1-\nu^2} \frac{\partial \left[ h(x) \frac{\partial h(x)}{\partial x} \phi_x \right]}{\partial x} + \frac{E_2 - cE_4}{2(1+\nu)} (h(x))^2 \frac{\partial^2 \phi_x}{\partial y^2}.$$

$$H_{15}(\phi_y) = \frac{E_2 - cE_4}{1-\nu^2} \nu \frac{\partial \left[ (h(x))^2 \frac{\partial \phi_y}{\partial y} \right]}{\partial x} + \frac{E_2 - cE_4}{2(1+\nu)} (h(x))^2 \frac{\partial^2 \phi_y}{\partial x \partial y} + \frac{cE_4}{1+\nu} h(x) \frac{\partial h(x)}{\partial x} \frac{\partial \phi_y}{\partial y},$$

### Appendix B

$$\bar{I}_1 = I_1 h(x) + \frac{2I_2}{a} (h(x))^2, \quad \bar{I}'_1 = I_1 h(x) + \frac{2I_2}{R} (h(x))^2,$$

$$\bar{I}_2 = \left( I_2 - \frac{4}{3}I_4 \right) (h(x))^2 + \left( I_3 - \frac{4}{3}I_5 \right) \frac{(h(x))^3}{a},$$

$$\bar{I}'_2 = \left( I_2 - \frac{4}{3}I_4 \right) (h(x))^2 + \left( I_3 - \frac{4}{3}I_5 \right) \frac{(h(x))^3}{R}, \quad \bar{I}_3 = \frac{4I_4}{3} (h(x))^2 + \frac{4I_5}{3a} (h(x))^3,$$

$$\bar{I}_4 = \bar{I}'_4 = \left( I_3 - \frac{8I_5}{3} + \frac{16}{9}I_7 \right) (h(x))^3,$$

$$H_{21}(u_0) = \frac{E_1 \nu}{1-\nu^2} h(x) \frac{\partial^2 u_0}{\partial x \partial y} + \frac{E_1}{2(1+\nu)} \frac{\partial \left[ h(x) \frac{\partial u_0}{\partial y} \right]}{\partial x}.$$

$$H_{22}(v_0) = \frac{E_1}{1-\nu^2} h(x) \frac{\partial^2 v_0}{\partial y^2} + \frac{E_1}{2(1+\nu)} \frac{\partial \left[ h(x) \frac{\partial v_0}{\partial x} \right]}{\partial x}.$$

$$H_{23}(w_0) = H_{23a}(w_0) + H_{23b}(w_0).$$

$$H_{23a}(w_0) = -\frac{E_1}{1-\nu^2} \left( \frac{1}{R} + \frac{\nu}{a} \right) h(x) \frac{\partial w_0}{\partial y} - \frac{cE_4}{1-\nu^2} (h(x))^2 \left( \frac{\partial^3 w_0}{\partial y^3} + \nu \frac{\partial^3 w_0}{\partial x^2 \partial y} \right) \\ - \frac{cE_4}{1+\nu} \frac{\partial \left[ (h(x))^2 \frac{\partial^2 w_0}{\partial x \partial y} \right]}{\partial x} + \frac{2cE_4 \nu}{1-\nu^2} h(x) \frac{\partial h(x)}{\partial x} \frac{\partial^2 w_0}{\partial x \partial y} + \frac{cE_4}{1+\nu} \frac{\partial \left[ h(x) \frac{\partial h(x)}{\partial x} \frac{\partial w_0}{\partial y} \right]}{\partial x}.$$

$$H_{23b}(w_0) = \frac{E_1}{1-\nu^2} h(x) \left( \frac{\partial w_0}{\partial y} \frac{\partial^2 w_0}{\partial y^2} + \nu \frac{\partial w_0}{\partial x} \frac{\partial^2 w_0}{\partial x \partial y} \right) + \frac{E_1}{2(1+\nu)} \frac{\partial \left[ h(x) \frac{\partial w_0}{\partial x} \frac{\partial w_0}{\partial y} \right]}{\partial x}.$$

$$H_{24}(\phi_x) = \frac{(E_2 - cE_4)\nu}{1-\nu^2} (h(x))^2 \frac{\partial^2 \phi_x}{\partial x \partial y} + \frac{E_2 - cE_4}{2(1+\nu)} \frac{\partial \left[ (h(x))^2 \frac{\partial \phi_x}{\partial y} \right]}{\partial x} + \frac{2cE_4 \nu}{1-\nu^2} h(x) \frac{\partial h(x)}{\partial x} \frac{\partial \phi_x}{\partial y}.$$

$$H_{25}(\phi_y) = \frac{E_2 - cE_4}{1-\nu^2} (h(x))^2 \frac{\partial^2 \phi_y}{\partial y^2} + \frac{E_2 - cE_4}{2(1+\nu)} \frac{\partial \left[ (h(x))^2 \frac{\partial \phi_y}{\partial x} \right]}{\partial x} + \frac{cE_4}{1+\nu} \frac{\partial \left[ h(x) \frac{\partial h(x)}{\partial x} \phi_y \right]}{\partial x}.$$

$$H_{31}(u_0) = \frac{E_1 h(x)}{1-\nu^2} \left( \frac{1}{a} + \frac{\nu}{R} \right) \frac{\partial u_0}{\partial x} + \frac{cE_4}{1-\nu^2} \frac{\partial^2 \left[ (h(x))^4 \frac{\partial u_0}{\partial x} \right]}{\partial x^2} + \frac{cE_4}{1+\nu} \frac{\partial \left[ (h(x))^4 \frac{\partial^2 u_0}{\partial y^2} \right]}{\partial x} \\ + \frac{cE_4 \nu}{1-\nu^2} (h(x))^4 \frac{\partial^3 u_0}{\partial x \partial y^2}.$$

$$H_{32}(v_0) = \frac{E_1 h(x)}{1-\nu^2} \left( \frac{1}{R} + \frac{\nu}{a} \right) \frac{\partial v_0}{\partial y} + \frac{cE_4 \nu}{1-\nu^2} \frac{\partial^2 \left[ (h(x))^4 \frac{\partial v_0}{\partial y} \right]}{\partial x^2} + \frac{cE_4}{1+\nu} \frac{\partial \left[ (h(x))^4 \frac{\partial^2 v_0}{\partial x \partial y} \right]}{\partial x} \\ + \frac{cE_4 \nu}{1-\nu^2} (h(x))^4 \frac{\partial^3 v_0}{\partial y^3}.$$

$$H_{33}(w_0) = H_{33a}(w_0) + H_{33b}(w_0) + H_{33c}(w_0).$$

$$\begin{aligned}
 H_{33a}(w_0) = & \frac{E_1 - 3cE_3}{2(1 + \nu)} \left\{ \frac{\partial \left[ h(x) \frac{\partial w_0}{\partial x} \right]}{\partial x} + h(x) \frac{\partial^2 w_0}{\partial y^2} \right\} \\
 & - 3c \frac{E_3 - 3cE_5}{2(1 + \nu)} \left\{ \frac{\partial \left[ (h(x))^3 \frac{\partial w_0}{\partial x} \right]}{\partial x} + (h(x))^3 \frac{\partial^2 w_0}{\partial y^2} \right\} - \frac{E_1}{1 - \nu^2} \left( \frac{1}{R^2} + \frac{2\nu}{Ra} + \frac{1}{a^2} \right) h(x) w_0 \\
 & - \frac{cE_4}{1 - \nu^2} (h(x))^2 \left[ \left( \frac{1}{a} + \frac{\nu}{R} \right) \frac{\partial^2 w_0}{\partial x^2} + \left( \frac{1}{R} + \frac{\nu}{a} \right) \frac{\partial^2 w_0}{\partial y^2} \right] - \frac{cE_4}{1 - \nu^2} \left( \frac{1}{a} + \frac{\nu}{R} \right) \frac{\partial^2 \left[ (h(x))^4 w_0 \right]}{\partial x^2} \\
 & - \frac{c^2 E_7}{1 - \nu^2} \frac{\partial^2 \left[ (h(x))^5 \left( \frac{\partial^2 w_0}{\partial x^2} + \nu \frac{\partial^2 w_0}{\partial y^2} \right) \right]}{\partial x^2} - \frac{c^2 E_7}{1 + \nu} \frac{\partial \left[ (h(x))^5 \frac{\partial^3 w_0}{\partial x \partial y^2} \right]}{\partial x} \\
 & - \frac{cE_4}{1 - \nu^2} \left( \frac{1}{R} + \frac{\nu}{a} \right) (h(x))^4 \frac{\partial^2 w_0}{\partial y^2} - \frac{c^2 E_7}{1 - \nu^2} (h(x))^5 \left( \frac{\partial^4 w_0}{\partial y^4} + \nu \frac{\partial^4 w_0}{\partial x^2 \partial y^2} \right) \\
 & + \frac{2c^2 E_7}{1 - \nu^2} \frac{\partial^2 \left[ (h(x))^4 \frac{\partial h(x)}{\partial x} \frac{\partial w_0}{\partial x} \right]}{\partial x^2} + \frac{2c^2 \nu E_7}{1 - \nu^2} (h(x))^4 \frac{\partial h(x)}{\partial x} \frac{\partial^3 w_0}{\partial x \partial y^2} \\
 & + \frac{2c^2 E_7}{1 + \nu} \frac{\partial \left[ (h(x))^4 \frac{\partial h(x)}{\partial x} \frac{\partial^2 w_0}{\partial y^2} \right]}{\partial x}.
 \end{aligned}$$

$$\begin{aligned}
 H_{33b}(w_0) = & \frac{E_1 h(x)}{2(1 - \nu^2)} \left[ \left( \frac{1}{a} + \frac{\nu}{R} \right) \left( \frac{\partial w_0}{\partial x} \right)^2 + \left( \frac{1}{R} + \frac{\nu}{a} \right) \left( \frac{\partial w_0}{\partial y} \right)^2 \right] \\
 & + \frac{cE_4}{2(1 - \nu^2)} \frac{\partial^2 \left[ (h(x))^4 \left( \left( \frac{\partial w_0}{\partial x} \right)^2 + \nu \left( \frac{\partial w_0}{\partial y} \right)^2 \right) \right]}{\partial x^2} \\
 & + \frac{cE_4}{1 + \nu} \frac{\partial \left[ (h(x))^4 \left( \frac{\partial w_0}{\partial x} \frac{\partial^2 w_0}{\partial y^2} + \frac{\partial w_0}{\partial y} \frac{\partial^2 w_0}{\partial x \partial y} \right) \right]}{\partial x} + \frac{cE_4}{2(1 - \nu^2)} (h(x))^4 \frac{\partial^2 \left( \left( \frac{\partial w_0}{\partial x} \right)^2 + \nu \left( \frac{\partial w_0}{\partial y} \right)^2 \right)}{\partial y^2} \\
 & - \frac{E_1 h(x) w_0}{1 - \nu^2} \left[ \left( \frac{1}{a} + \frac{\nu}{R} \right) \frac{\partial^2 w_0}{\partial x^2} + \left( \frac{1}{R} + \frac{\nu}{a} \right) \frac{\partial^2 w_0}{\partial y^2} \right] \\
 & - \frac{cE_4 (h(x))^2}{1 - \nu^2} \left( \left( \frac{\partial^2 w_0}{\partial x^2} \right)^2 + 2\nu \frac{\partial^2 w_0}{\partial x^2} \frac{\partial^2 w_0}{\partial y^2} + \left( \frac{\partial^2 w_0}{\partial y^2} \right)^2 \right) + \frac{2cE_4}{1 + \nu} (h(x))^2 \left( \frac{\partial^2 w_0}{\partial x \partial y^2} \right)^2 \\
 & + \frac{2cE_4}{1 - \nu^2} h(x) \frac{\partial h(x)}{\partial x} \frac{\partial w_0}{\partial x} \left( \frac{\partial^2 w_0}{\partial x^2} + \nu \frac{\partial^2 w_0}{\partial y^2} \right) + \frac{2cE_4}{1 + \nu} h(x) \frac{\partial h(x)}{\partial x} \frac{\partial w_0}{\partial y} \frac{\partial^2 w_0}{\partial x \partial y}.
 \end{aligned}$$

$$\begin{aligned}
 H_{33c}(w_0) = & \frac{E_1 h(x)}{2(1 - \nu^2)} \left[ \left( \left( \frac{\partial w_0}{\partial x} \right)^2 + \nu \left( \frac{\partial w_0}{\partial y} \right)^2 \right) \frac{\partial^2 w_0}{\partial x^2} + \left( \left( \frac{\partial w_0}{\partial y} \right)^2 + \nu \left( \frac{\partial w_0}{\partial x} \right)^2 \right) \frac{\partial^2 w_0}{\partial y^2} \right] \\
 & + \frac{E_1 h(x)}{1 + \nu} \frac{\partial w_0}{\partial x} \frac{\partial w_0}{\partial y} \frac{\partial^2 w_0}{\partial x \partial y}.
 \end{aligned}$$

$$\begin{aligned}
H_{34}(\phi_x) &= \frac{E_2 - cE_4}{1 - \nu^2} \left( \frac{1}{a} + \frac{\nu}{R} \right) (h(x))^2 \frac{\partial \phi_x}{\partial x} + \frac{c(E_5 - cE_7)}{1 - \nu^2} \frac{\partial^2 \left[ (h(x))^5 \frac{\partial \phi_x}{\partial x} \right]}{\partial x^2} \\
&\quad + \frac{c(E_5 - cE_7)}{1 + \nu} \frac{\partial \left[ (h(x))^5 \frac{\partial^2 \phi_x}{\partial y^2} \right]}{\partial x} + \frac{c\nu(E_5 - cE_7)}{1 - \nu^2} (h(x))^5 \frac{\partial^3 w_0}{\partial x \partial y^2} + \frac{E_1 - 3cE_3}{2(1 + \nu)} \frac{\partial [h(x)\phi_x]}{\partial x} \\
&\quad - 3c \frac{E_3 - 3cE_5}{2(1 + \nu)} \frac{\partial \left[ (h(x))^3 \phi_x \right]}{\partial x} + \frac{2c\nu E_4}{1 - \nu^2} \left( \frac{1}{a} + \frac{1}{R} \right) h(x) \frac{\partial h(x)}{\partial x} \phi_x \\
&\quad + \frac{2c^2 E_7}{1 - \nu^2} \frac{\partial^2 \left[ (h(x))^4 \frac{\partial h(x)}{\partial x} \phi_x \right]}{\partial x^2} + \frac{2c^2 \nu E_7}{1 - \nu^2} (h(x))^4 \frac{\partial h(x)}{\partial x} \frac{\partial^2 \phi_x}{\partial y^2}.
\end{aligned}$$

$$\begin{aligned}
H_{35}(\phi_y) &= \frac{E_2 - cE_4}{1 - \nu^2} \left( \frac{1}{R} + \frac{\nu}{a} \right) (h(x))^2 \frac{\partial \phi_y}{\partial y} + \frac{c\nu(E_5 - cE_7)}{1 - \nu^2} \frac{\partial^2 \left[ (h(x))^5 \frac{\partial \phi_y}{\partial y} \right]}{\partial x^2} \\
&\quad + \frac{c(E_5 - cE_7)}{1 + \nu} \frac{\partial \left[ (h(x))^5 \frac{\partial^2 \phi_y}{\partial x \partial y} \right]}{\partial x} + \frac{c\nu(E_5 - cE_7)}{1 - \nu^2} (h(x))^5 \frac{\partial^3 \phi_y}{\partial y^3} + \frac{E_1 - 3cE_3}{2(1 + \nu)} h(x) \frac{\partial \phi_y}{\partial y} \\
&\quad - 3c \frac{E_3 - 3cE_5}{2(1 + \nu)} (h(x))^3 \frac{\partial \phi_y}{\partial y} + \frac{2c^2 E_7}{1 + \nu} \frac{\partial \left[ (h(x))^4 \frac{\partial h(x)}{\partial x} \frac{\partial \phi_y}{\partial y} \right]}{\partial x}.
\end{aligned}$$

$$H_{36}(u_0, w_0) = \frac{E_1 h(x)}{1 - \nu^2} \frac{\partial u_0}{\partial x} \left( \frac{\partial^2 w_0}{\partial x^2} + \nu \frac{\partial^2 w_0}{\partial y^2} \right) - \frac{2cE_7}{1 + \nu} h(x) \frac{\partial u_0}{\partial y} \frac{\partial^2 w_0}{\partial x \partial y}.$$

$$H_{37}(v_0, w_0) = \frac{E_1 h(x)}{1 - \nu^2} \frac{\partial v_0}{\partial y} \left( \frac{\partial^2 w_0}{\partial y^2} + \nu \frac{\partial^2 w_0}{\partial x^2} \right) - \frac{2cE_7}{1 + \nu} h(x) \frac{\partial v_0}{\partial x} \frac{\partial^2 w_0}{\partial x \partial y}.$$

$$\begin{aligned}
H_{38}(\phi_x, w_0) &= \frac{E_2 - cE_4}{1 - \nu^2} (h(x))^2 \frac{\partial \phi_x}{\partial x} \left( \frac{\partial^2 w_0}{\partial x^2} + \nu \frac{\partial^2 w_0}{\partial y^2} \right) + \frac{E_2 - cE_4}{1 + \nu} (h(x))^2 \frac{\partial \phi_x}{\partial y} \frac{\partial^2 w_0}{\partial x \partial y} \\
&\quad + \frac{2cE_4}{1 - \nu^2} h(x) \frac{\partial h(x)}{\partial x} \phi_x \left( \frac{\partial^2 w_0}{\partial x^2} + \nu \frac{\partial^2 w_0}{\partial y^2} \right).
\end{aligned}$$

$$\begin{aligned}
H_{39}(\phi_y, w_0) &= \frac{E_2 - cE_4}{1 - \nu^2} (h(x))^2 \frac{\partial \phi_y}{\partial y} \left( \frac{\partial^2 w_0}{\partial y^2} + \nu \frac{\partial^2 w_0}{\partial x^2} \right) + \frac{E_2 - cE_4}{1 + \nu} (h(x))^2 \frac{\partial \phi_y}{\partial x} \frac{\partial^2 w_0}{\partial x \partial y} \\
&\quad + \frac{2cE_4}{1 + \nu} h(x) \frac{\partial h(x)}{\partial x} \frac{\partial^2 w_0}{\partial x \partial y} \phi_y.
\end{aligned}$$

$$\begin{aligned}
H_{41}(u_0) &= \frac{E_2}{1 - \nu^2} \frac{\partial \left[ (h(x))^2 \frac{\partial u_0}{\partial x} \right]}{\partial x} + \frac{E_2}{2(1 + \nu)} (h(x))^2 \frac{\partial^2 u_0}{\partial y^2} - \frac{cE_4}{1 - \nu^2} \frac{\partial \left[ (h(x))^4 \frac{\partial u_0}{\partial x} \right]}{\partial x} \\
&\quad - \frac{cE_4}{2(1 + \nu)} (h(x))^4 \frac{\partial^2 u_0}{\partial y^2}.
\end{aligned}$$

$$H_{42}(v_0) = \frac{\nu E_2}{1 - \nu^2} \frac{\partial \left[ (h(x))^2 \frac{\partial v_0}{\partial y} \right]}{\partial x} + \frac{E_2}{2(1 + \nu)} (h(x))^2 \frac{\partial^2 v_0}{\partial x \partial y} - \frac{c \nu E_4}{1 - \nu^2} \frac{\partial \left[ (h(x))^4 \frac{\partial v_0}{\partial y} \right]}{\partial x} - \frac{c E_4}{2(1 + \nu)} (h(x))^4 \frac{\partial^2 v_0}{\partial x \partial y}.$$

$$H_{43}(w_0) = H_{43a}(w_0) + H_{43b}(w_0).$$

$$H_{43a}(w_0) = \frac{-E_2}{1 - \nu^2} \left( \frac{1}{a} + \frac{\nu}{R} \right) \frac{\partial \left[ (h(x))^2 w_0 \right]}{\partial x} - \frac{c E_5}{1 - \nu^2} \frac{\partial \left[ (h(x))^3 \left( \frac{\partial^2 w_0}{\partial x^2} + \nu \frac{\partial^2 w_0}{\partial y^2} \right) \right]}{\partial x} - \frac{c E_5}{1 + \nu} (h(x))^3 \frac{\partial^3 w_0}{\partial x \partial y^2} + \left[ -\frac{E_1 - 3c E_3}{2(1 + \nu)} h(x) + 3c \frac{E_3 - 3c E_5}{2(1 + \nu)} (h(x))^3 \right] \frac{\partial w_0}{\partial x} + \frac{c E_4}{1 - \nu^2} \left( \frac{1}{a} + \frac{\nu}{R} \right) \frac{\partial \left[ (h(x))^4 w_0 \right]}{\partial x} + \frac{c^2 E_7}{1 - \nu^2} \frac{\partial \left[ (h(x))^5 \left( \frac{\partial^2 w_0}{\partial x^2} + \nu \frac{\partial^2 w_0}{\partial y^2} \right) \right]}{\partial x} + \frac{c^2 E_7}{1 + \nu} (h(x))^5 \frac{\partial^3 w_0}{\partial x \partial y^2} + \frac{2c E_5}{1 - \nu^2} \frac{\partial \left[ (h(x))^2 \frac{\partial h(x)}{\partial x} \frac{\partial w_0}{\partial x} \right]}{\partial x} + \frac{c E_5}{1 + \nu} (h(x))^2 \frac{\partial h(x)}{\partial x} \frac{\partial^2 w_0}{\partial y^2} - \frac{2c^2 E_7}{1 - \nu^2} \frac{\partial \left[ (h(x))^4 \frac{\partial h(x)}{\partial x} \frac{\partial w_0}{\partial x} \right]}{\partial x} - \frac{c^2 E_7}{1 + \nu} (h(x))^4 \frac{\partial h(x)}{\partial x} \frac{\partial^2 w_0}{\partial y^2}.$$

$$H_{43b}(w_0) = \frac{E_2 h(x)}{2(1 - \nu^2)} \frac{\partial \left[ (h(x))^2 \left( \left( \frac{\partial w_0}{\partial x} \right)^2 + \nu \left( \frac{\partial w_0}{\partial y} \right)^2 \right) \right]}{\partial x} + \frac{E_2 (h(x))^2}{2(1 + \nu)} \frac{\partial \left( \frac{\partial w_0}{\partial x} \frac{\partial w_0}{\partial y} \right)}{\partial y} - \frac{c E_4}{2(1 - \nu^2)} \frac{\partial \left[ (h(x))^4 \left( \left( \frac{\partial w_0}{\partial x} \right)^2 + \nu \left( \frac{\partial w_0}{\partial y} \right)^2 \right) \right]}{\partial x} - \frac{c E_4 (h(x))^4}{2(1 + \nu)} \frac{\partial \left( \frac{\partial w_0}{\partial x} \frac{\partial w_0}{\partial y} \right)}{\partial y}.$$

$$H_{44}(\phi_x) = \frac{E_3 - c E_5}{1 - \nu^2} \frac{\partial \left[ (h(x))^3 \frac{\partial \phi_x}{\partial x} \right]}{\partial x} + \frac{E_3 - c E_5}{2(1 + \nu)} (h(x))^3 \frac{\partial^2 \phi_x}{\partial y^2} + \left[ -\frac{E_1 - 3c E_3}{2(1 + \nu)} h(x) + 3c \frac{E_3 - 3c E_5}{2(1 + \nu)} (h(x))^3 \right] \phi_x - c \frac{E_5 - c E_7}{1 - \nu^2} \frac{\partial \left[ (h(x))^5 \frac{\partial \phi_x}{\partial x} \right]}{\partial x} - c \frac{E_5 - c E_7}{2(1 + \nu)} (h(x))^5 \frac{\partial^2 \phi_x}{\partial y^2} + \frac{2c E_5}{1 - \nu^2} \frac{\partial \left[ (h(x))^2 \frac{\partial h(x)}{\partial x} \phi_x \right]}{\partial x} - \frac{2c^2 E_7}{1 - \nu^2} \frac{\partial \left[ (h(x))^4 \frac{\partial h(x)}{\partial x} \phi_x \right]}{\partial x}.$$

$$H_{45}(\phi_y) = \nu \frac{E_3 - c E_5}{1 - \nu^2} \frac{\partial \left[ (h(x))^3 \frac{\partial \phi_y}{\partial y} \right]}{\partial x} + \frac{E_3 - c E_5}{2(1 + \nu)} (h(x))^3 \frac{\partial^2 \phi_y}{\partial x \partial y} - c \nu \frac{E_5 - c E_7}{1 - \nu^2} \frac{\partial \left[ (h(x))^5 \frac{\partial \phi_y}{\partial y} \right]}{\partial x} + \frac{c E_5}{1 + \nu} (h(x))^2 \frac{\partial h(x)}{\partial x} \frac{\partial \phi_y}{\partial y} - \frac{c^2 E_7}{1 + \nu} (h(x))^4 \frac{\partial h(x)}{\partial x} \frac{\partial \phi_y}{\partial y}.$$



$$H_{51}(u_0) = \frac{E_2}{2(1+\nu)} \frac{\partial \left[ (h(x))^2 \frac{\partial u_0}{\partial y} \right]}{\partial x} + \frac{\nu E_2}{1-\nu^2} (h(x))^2 \frac{\partial^2 u_0}{\partial x \partial y} - \frac{cE_4}{2(1+\nu)} \frac{\partial \left[ (h(x))^4 \frac{\partial u_0}{\partial y} \right]}{\partial x} - \frac{c\nu E_4}{1-\nu^2} (h(x))^4 \frac{\partial^2 u_0}{\partial x \partial y}.$$

$$H_{52}(v_0) = \frac{E_2}{2(1+\nu)} \frac{\partial \left[ (h(x))^2 \frac{\partial v_0}{\partial x} \right]}{\partial x} + \frac{E_2}{1-\nu^2} (h(x))^2 \frac{\partial^2 v_0}{\partial y^2} - \frac{cE_4}{2(1+\nu)} \frac{\partial \left[ (h(x))^4 \frac{\partial v_0}{\partial x} \right]}{\partial x} - \frac{cE_4}{1-\nu^2} (h(x))^4 \frac{\partial^2 v_0}{\partial y^2}.$$

$$H_{53a}(w_0) = -\frac{cE_5}{1+\nu} \frac{\partial \left[ (h(x))^3 \frac{\partial^2 w_0}{\partial x \partial y} \right]}{\partial x} - \frac{E_2}{1-\nu^2} \left( \frac{1}{R} + \frac{\nu}{a} \right) (h(x))^2 \frac{\partial w_0}{\partial y} - \frac{cE_5}{1-\nu^2} (h(x))^3 \left( \frac{\partial^3 w_0}{\partial y^3} + \nu \frac{\partial^3 w_0}{\partial x^2 \partial y} \right) + \left[ -\frac{E_1 - 3cE_3}{2(1+\nu)} h(x) + 3c \frac{E_3 - 3cE_5}{2(1+\nu)} (h(x))^3 \right] \frac{\partial w_0}{\partial y} + \frac{c^2 E_7}{1+\nu} \frac{\partial \left[ (h(x))^5 \frac{\partial^2 w_0}{\partial x \partial y} \right]}{\partial x} + \frac{cE_4}{1-\nu^2} \left( \frac{1}{R} + \frac{\nu}{a} \right) (h(x))^4 \frac{\partial w_0}{\partial y} + \frac{c^2 E_7}{1-\nu^2} (h(x))^5 \left( \frac{\partial^3 w_0}{\partial y^3} + \nu \frac{\partial^3 w_0}{\partial x^2 \partial y} \right) + \frac{cE_5}{1+\nu} \frac{\partial \left[ (h(x))^2 \frac{\partial h(x)}{\partial x} \frac{\partial w_0}{\partial y} \right]}{\partial x} + \frac{2c\nu E_5}{1-\nu^2} (h(x))^2 \frac{\partial h(x)}{\partial x} \frac{\partial^2 w_0}{\partial x \partial y} - \frac{c^2 E_7}{1+\nu} \frac{\partial \left[ (h(x))^4 \frac{\partial h(x)}{\partial x} \frac{\partial w_0}{\partial y} \right]}{\partial x} - \frac{2\nu c^2 E_7}{1-\nu^2} (h(x))^4 \frac{\partial h(x)}{\partial x} \frac{\partial^2 w_0}{\partial x \partial y}.$$

$$H_{53b}(w_0) = \frac{E_2}{2(1+\nu)} \frac{\partial \left[ (h(x))^2 \frac{\partial w_0}{\partial x} \frac{\partial w_0}{\partial y} \right]}{\partial x} + \frac{E_2 (h(x))^2}{2(1-\nu^2)} \frac{\partial \left( \left( \frac{\partial w_0}{\partial y} \right)^2 + \nu \left( \frac{\partial w_0}{\partial x} \right)^2 \right)}{\partial y} - \frac{cE_4 (h(x))^4}{2(1+\nu)} \frac{\partial \left( \left( \frac{\partial w_0}{\partial y} \right)^2 + \nu \left( \frac{\partial w_0}{\partial x} \right)^2 \right)}{\partial y},$$

$$H_{54}(\phi_x) = \frac{E_3 - cE_5}{2(1+\nu)} \frac{\partial \left[ (h(x))^3 \frac{\partial \phi_x}{\partial y} \right]}{\partial x} + \nu \frac{E_3 - cE_5}{1-\nu^2} (h(x))^3 \frac{\partial^2 \phi_x}{\partial x \partial y} - c \frac{E_5 - cE_7}{2(1+\nu)} \frac{\partial \left[ (h(x))^5 \frac{\partial \phi_x}{\partial y} \right]}{\partial x} - c\nu \frac{E_5 - cE_7}{1-\nu^2} (h(x))^5 \frac{\partial^2 \phi_x}{\partial x \partial y} + \frac{2\nu cE_5}{1-\nu^2} (h(x))^2 \frac{\partial h(x)}{\partial x} \frac{\partial \phi_x}{\partial y}.$$

$$\begin{aligned}
 H_{55}(\phi_y) &= \frac{E_3 - cE_5}{2(1 + \nu)} \frac{\partial \left[ (h(x))^3 \frac{\partial \phi_y}{\partial x} \right]}{\partial x} + \frac{E_3 - cE_5}{1 - \nu^2} (h(x))^3 \frac{\partial^2 \phi_y}{\partial y^2} \\
 &+ \left[ -\frac{E_1 - 3cE_3}{2(1 + \nu)} h(x) + 3c \frac{E_3 - 3cE_5}{2(1 + \nu)} (h(x))^3 \right] \phi_y - c \frac{E_5 - cE_7}{2(1 + \nu)} \frac{\partial \left[ (h(x))^5 \frac{\partial \phi_y}{\partial x} \right]}{\partial x} \\
 &+ \frac{cE_5}{1 + \nu} \frac{\partial \left[ (h(x))^2 \frac{\partial h(x)}{\partial x} \phi_y \right]}{\partial x} - c \frac{E_5 - cE_7}{1 - \nu^2} (h(x))^5 \frac{\partial^2 \phi_y}{\partial y^2} - \frac{c^2 E_7}{1 + \nu} \frac{\partial \left[ (h(x))^4 \frac{\partial h(x)}{\partial x} \phi_y \right]}{\partial x}. \quad c = \frac{4}{3}.
 \end{aligned}$$

**Appendix D**

$$\begin{aligned}
 l_{11}U &= \int_0^L \int_0^{2\pi R} H_{11}(u_0) \cos \frac{m\pi x}{L} \sin \frac{ny}{R} dx dy, \\
 l_{12}V &= \int_0^L \int_0^{2\pi R} H_{12}(v_0) \cos \frac{m\pi x}{L} \sin \frac{ny}{R} dx dy, \\
 l_{13}W &= \int_0^L \int_0^{2\pi R} H_{13a}(w_0) \cos \frac{m\pi x}{L} \sin \frac{ny}{R} dx dy, \\
 l_{14}\Phi_x &= \int_0^L \int_0^{2\pi R} H_{14}(\phi_x) \cos \frac{m\pi x}{L} \sin \frac{ny}{R} dx dy, \\
 l_{15}\Phi_y &= \int_0^L \int_0^{2\pi R} H_{15}(\phi_y) \cos \frac{m\pi x}{L} \sin \frac{ny}{R} dx dy, \\
 l_{16}W^2 &= \int_0^L \int_0^{2\pi R} H_{13b}(w_0) \cos \frac{m\pi x}{L} \sin \frac{ny}{R} dx dy, \\
 l_{17}\ddot{U} &= \int_0^L \int_0^{2\pi R} I_1 \ddot{u} \cos \frac{m\pi x}{L} \sin \frac{ny}{R} dx dy, \\
 l_{18}\ddot{\Phi}_x &= \int_0^L \int_0^{2\pi R} I_2 \ddot{\phi}_x \cos \frac{m\pi x}{L} \sin \frac{ny}{R} dx dy, \\
 l_{19}\ddot{W} &= - \int_0^L \int_0^{2\pi R} I_3 \frac{\partial \ddot{w}_0}{\partial x} \cos \frac{m\pi x}{L} \sin \frac{ny}{R} dx dy, \\
 l_{21}U &= \int_0^L \int_0^{2\pi R} H_{21}(u_0) \sin \frac{m\pi x}{L} \cos \frac{ny}{R} dx dy, \\
 l_{22}V &= \int_0^L \int_0^{2\pi R} H_{22}(v_0) \sin \frac{m\pi x}{L} \cos \frac{ny}{R} dx dy, \\
 l_{23}W &= \int_0^L \int_0^{2\pi R} H_{23a}(w_0) \sin \frac{m\pi x}{L} \cos \frac{ny}{R} dx dy, \\
 l_{24}\Phi_x &= \int_0^L \int_0^{2\pi R} H_{24}(\phi_x) \sin \frac{m\pi x}{L} \cos \frac{ny}{R} dx dy, \\
 l_{25}\Phi_y &= \int_0^L \int_0^{2\pi R} H_{25}(\phi_y) \sin \frac{m\pi x}{L} \cos \frac{ny}{R} dx dy, \\
 l_{26}W^2 &= \int_0^L \int_0^{2\pi R} H_{23b}(w_0) \sin \frac{m\pi x}{L} \cos \frac{ny}{R} dx dy, \\
 l_{27}\ddot{V} &= \int_0^L \int_0^{2\pi R} I_1' \ddot{v}_0 \sin \frac{m\pi x}{L} \cos \frac{ny}{R} dx dy, \\
 l_{28}\ddot{\Phi}_y &= \int_0^L \int_0^{2\pi R} I_2' \ddot{\phi}_y \sin \frac{m\pi x}{L} \cos \frac{ny}{R} dx dy,
 \end{aligned}$$

$$\begin{aligned}
 l_{29}\ddot{W} &= - \int_0^L \int_0^{2\pi R} I_3' \frac{\partial \ddot{w}_0}{\partial y} \sin \frac{m\pi x}{L} \cos \frac{ny}{R} dx dy, \\
 l_{31}U &= \int_0^L \int_0^{2\pi R} H_{31}(u_0) \sin \frac{m\pi x}{L} \sin \frac{ny}{R} dx dy, \\
 l_{32}V &= \int_0^L \int_0^{2\pi R} H_{32}(v_0) \sin \frac{m\pi x}{L} \sin \frac{ny}{R} dx dy, \\
 l_{33}W &= \int_0^L \int_0^{2\pi R} H_{33a}(w_0) \sin \frac{m\pi x}{L} \sin \frac{ny}{R} dx dy, \\
 l_{34}\Phi_x &= \int_0^L \int_0^{2\pi R} H_{34}(\phi_x) \sin \frac{m\pi x}{L} \sin \frac{ny}{R} dx dy, \\
 l_{35}\Phi_y &= \int_0^L \int_0^{2\pi R} H_{35}(\phi_y) \sin \frac{m\pi x}{L} \sin \frac{ny}{R} dx dy, \\
 l_{36}UW &= \int_0^L \int_0^{2\pi R} H_{36}(u_0, w_0) \sin \frac{m\pi x}{L} \sin \frac{ny}{R} dx dy, \\
 l_{37}VW &= \int_0^L \int_0^{2\pi R} H_{37}(v_0, w_0) \sin \frac{m\pi x}{L} \sin \frac{ny}{R} dx dy, \\
 l_{38}\Phi_x W &= \int_0^L \int_0^{2\pi R} H_{38}(\phi_x, w_0) \sin \frac{m\pi x}{L} \sin \frac{ny}{R} dx dy, \\
 l_{39}\Phi_y W &= \int_0^L \int_0^{2\pi R} H_{39}(\phi_y, w_0) \sin \frac{m\pi x}{L} \sin \frac{ny}{R} dx dy, \\
 l_{310}W^2 &= \int_0^L \int_0^{2\pi R} H_{33b}(w_0) \sin \frac{m\pi x}{L} \sin \frac{ny}{R} dx dy, \\
 l_{311}W^3 &= \int_0^L \int_0^{2\pi R} H_{33c}(w_0) \sin \frac{m\pi x}{L} \sin \frac{ny}{R} dx dy, \\
 l_{312} &= \int_0^L \int_0^{2\pi R} \sin \frac{m\pi x}{L} \sin \frac{ny}{R} dx dy \\
 l_{313}\ddot{U} &= \int_0^L \int_0^{2\pi R} I_3 \frac{\partial \ddot{u}_0}{\partial x} \sin \frac{m\pi x}{L} \sin \frac{ny}{R} dx dy, \\
 l_{314}\ddot{V} &= \int_0^L \int_0^{2\pi R} I_3' \frac{\partial \ddot{v}_0}{\partial y} \sin \frac{m\pi x}{L} \sin \frac{ny}{R} dx dy, \\
 l_{315}\ddot{\Phi}_x &= \int_0^L \int_0^{2\pi R} I_5 \frac{\partial \ddot{\phi}_x}{\partial x} \sin \frac{m\pi x}{L} \sin \frac{ny}{R} dx dy, \\
 l_{316}\ddot{\Phi}_y &= \int_0^L \int_0^{2\pi R} I_5' \frac{\partial \ddot{\phi}_y}{\partial y} \sin \frac{m\pi x}{L} \sin \frac{ny}{R} dx dy, \\
 l_{317}\ddot{W} &= \int_0^L \int_0^{2\pi R} \left[ I_1 h(x) \ddot{w}_0 - \frac{16h^3(x)}{9} I_7 \left( \frac{\partial^2 \ddot{w}_0}{\partial x^2} + \frac{\partial^2 \ddot{w}_0}{\partial y^2} \right) \right]
 \end{aligned}$$

$$\begin{aligned} & \sin \frac{m\pi x}{L} \sin \frac{ny}{R} dx dy, \\ l_{318} \dot{W} &= \int_0^L \int_0^{2\pi R} 2\epsilon I_1 h(x) \dot{w}_0 \sin \frac{m\pi x}{L} \sin \frac{ny}{R} dx dy, \\ l_{41} U &= \int_0^L \int_0^{2\pi R} H_{41}(u_0) \cos \frac{m\pi x}{L} \sin \frac{ny}{R} dx dy, \\ l_{42} V &= \int_0^L \int_0^{2\pi R} H_{42}(v_0) \cos \frac{m\pi x}{L} \sin \frac{ny}{R} dx dy, \\ l_{43} W &= \int_0^L \int_0^{2\pi R} H_{43a}(w_0) \cos \frac{m\pi x}{L} \sin \frac{ny}{R} dx dy, \\ l_{44} \Phi_x &= \int_0^L \int_0^{2\pi R} H_{44}(\phi_x) \cos \frac{m\pi x}{L} \sin \frac{ny}{R} dx dy, \end{aligned}$$

$$D_3 = \frac{l_{31}H_{12} + l_{32}H_{22} + l_{34}H_{32} + l_{35}H_{42} + l_{37}H_{11} + l_{38}H_{21} + l_{39}H_{31} + l_{310}H_{41}}{l_{31}H_{13} + l_{32}H_{23} + l_{34}H_{33} + l_{35}H_{43} - l_{317}},$$

$$\begin{aligned} l_{45} \Phi_y &= \int_0^L \int_0^{2\pi R} H_{45}(\phi_y) \cos \frac{m\pi x}{L} \sin \frac{ny}{R} dx dy, \\ l_{46} W^2 &= \int_0^L \int_0^{2\pi R} H_{43b}(w_0) \cos \frac{m\pi x}{L} \sin \frac{ny}{R} dx dy, \\ l_{47} \ddot{U} &= \int_0^L \int_0^{2\pi R} \bar{I}_2 \ddot{u}_0 \cos \frac{m\pi x}{L} \sin \frac{ny}{R} dx dy, \\ l_{48} \ddot{\Phi}_x &= \int_0^L \int_0^{2\pi R} \bar{I}_4 \ddot{\phi}_x \cos \frac{m\pi x}{L} \sin \frac{ny}{R} dx dy, \\ l_{49} \ddot{W} &= - \int_0^L \int_0^{2\pi R} \bar{I}_5 \frac{\partial \ddot{w}_0}{\partial x} \cos \frac{m\pi x}{L} \sin \frac{ny}{R} dx dy, \\ l_{51} U &= \int_0^L \int_0^{2\pi R} H_{51}(u_0) \sin \frac{m\pi x}{L} \cos \frac{ny}{R} dx dy, \\ l_{52} V &= \int_0^L \int_0^{2\pi R} H_{52}(v_0) \sin \frac{m\pi x}{L} \cos \frac{ny}{R} dx dy, \\ l_{53} W &= \int_0^L \int_0^{2\pi R} H_{53a}(w_0) \sin \frac{m\pi x}{L} \cos \frac{ny}{R} dx dy, \\ l_{54} \Phi_x &= \int_0^L \int_0^{2\pi R} H_{54}(\phi_x) \sin \frac{m\pi x}{L} \cos \frac{ny}{R} dx dy, \\ l_{55} \Phi_y &= \int_0^L \int_0^{2\pi R} H_{55}(\phi_y) \sin \frac{m\pi x}{L} \cos \frac{ny}{R} dx dy, \\ l_{56} W^2 &= \int_0^L \int_0^{2\pi R} H_{53b}(w_0) \sin \frac{m\pi x}{L} \cos \frac{ny}{R} dx dy, \\ l_{57} \ddot{V} &= \int_0^L \int_0^{2\pi R} \bar{I}'_2 \ddot{v}_0 \sin \frac{m\pi x}{L} \cos \frac{ny}{R} dx dy, \end{aligned}$$

$$\begin{aligned} l_{58} \ddot{\Phi}_y &= \int_0^L \int_0^{2\pi R} \bar{I}'_4 \ddot{\phi}_y \sin \frac{m\pi x}{L} \cos \frac{ny}{R} dx dy, \\ l_{59} \ddot{W} &= - \int_0^L \int_0^{2\pi R} \bar{I}'_5 \frac{\partial \ddot{w}_0}{\partial y} \sin \frac{m\pi x}{L} \cos \frac{ny}{R} dx dy. \end{aligned}$$

### Appendix E

$$D_1 = \frac{l_{37}H_{13} + l_{38}H_{23} + l_{39}H_{33} + l_{310}H_{43}}{l_{31}H_{13} + l_{32}H_{23} + l_{34}H_{33} + l_{35}H_{43} - l_{317}},$$

$$D_2 = \frac{l_{31}H_{11} + l_{32}H_{21} + l_{33} + l_{34}H_{31} + l_{35}H_{41}}{l_{31}H_{13} + l_{32}H_{23} + l_{34}H_{33} + l_{35}H_{43} - l_{317}},$$

$$D_4 = \frac{l_{37}H_{12} + l_{38}H_{22} + l_{39}H_{32} + l_{310}H_{42} + l_{311}}{l_{31}H_{13} + l_{32}H_{23} + l_{34}H_{33} + l_{35}H_{43} - l_{317}},$$

$$D_5 = \frac{l_{312}}{l_{31}H_{13} + l_{32}H_{23} + l_{34}H_{33} + l_{35}H_{43} - l_{317}},$$

in which

$$\begin{aligned} H_{11} &= \frac{-\det \begin{pmatrix} l_{13} & l_{12} & l_{14} & l_{15} \\ l_{23} & l_{22} & l_{24} & l_{25} \\ l_{43} & l_{42} & l_{44} & l_{45} \\ l_{53} & l_{52} & l_{54} & l_{55} \end{pmatrix}}{\Delta}, & H_{12} &= \frac{-\det \begin{pmatrix} l_{16} & l_{12} & l_{14} & l_{15} \\ l_{26} & l_{22} & l_{24} & l_{25} \\ l_{46} & l_{42} & l_{44} & l_{45} \\ l_{56} & l_{52} & l_{54} & l_{55} \end{pmatrix}}{\Delta}, \\ H_{13} &= \frac{\det \begin{pmatrix} l_{19} & l_{12} & l_{14} & l_{15} \\ l_{29} & l_{22} & l_{24} & l_{25} \\ l_{49} & l_{42} & l_{44} & l_{45} \\ l_{59} & l_{52} & l_{54} & l_{55} \end{pmatrix}}{\Delta}, & H_{21} &= \frac{-\det \begin{pmatrix} l_{11} & l_{13} & l_{14} & l_{15} \\ l_{21} & l_{23} & l_{24} & l_{25} \\ l_{41} & l_{43} & l_{44} & l_{45} \\ l_{51} & l_{53} & l_{54} & l_{55} \end{pmatrix}}{\Delta}, \\ H_{13} &= \frac{-\det \begin{pmatrix} l_{11} & l_{16} & l_{14} & l_{15} \\ l_{21} & l_{26} & l_{24} & l_{25} \\ l_{41} & l_{46} & l_{44} & l_{45} \\ l_{51} & l_{56} & l_{54} & l_{55} \end{pmatrix}}{\Delta}, & H_{21} &= \frac{\det \begin{pmatrix} l_{11} & l_{19} & l_{14} & l_{15} \\ l_{21} & l_{29} & l_{24} & l_{25} \\ l_{41} & l_{49} & l_{44} & l_{45} \\ l_{51} & l_{59} & l_{54} & l_{55} \end{pmatrix}}{\Delta}, \\ H_{22} &= \frac{-\det \begin{pmatrix} l_{11} & l_{12} & l_{13} & l_{15} \\ l_{21} & l_{22} & l_{23} & l_{25} \\ l_{41} & l_{42} & l_{43} & l_{45} \\ l_{51} & l_{52} & l_{53} & l_{55} \end{pmatrix}}{\Delta}, & H_{23} &= \frac{\det \begin{pmatrix} l_{11} & l_{12} & l_{16} & l_{15} \\ l_{21} & l_{22} & l_{26} & l_{25} \\ l_{41} & l_{42} & l_{46} & l_{45} \\ l_{51} & l_{52} & l_{56} & l_{55} \end{pmatrix}}{\Delta}, \\ H_{31} &= \frac{-\det \begin{pmatrix} l_{11} & l_{12} & l_{13} & l_{15} \\ l_{21} & l_{22} & l_{23} & l_{25} \\ l_{41} & l_{42} & l_{43} & l_{45} \\ l_{51} & l_{52} & l_{53} & l_{55} \end{pmatrix}}{\Delta}, & H_{32} &= \frac{-\det \begin{pmatrix} l_{11} & l_{12} & l_{16} & l_{15} \\ l_{21} & l_{22} & l_{26} & l_{25} \\ l_{41} & l_{42} & l_{46} & l_{45} \\ l_{51} & l_{52} & l_{56} & l_{55} \end{pmatrix}}{\Delta}, \end{aligned}$$

$$H_{33} = \frac{\det \begin{pmatrix} l_{11} & l_{12} & l_{19} & l_{15} \\ l_{21} & l_{22} & l_{29} & l_{25} \\ l_{41} & l_{42} & l_{49} & l_{45} \\ l_{51} & l_{52} & l_{59} & l_{55} \end{pmatrix}}{\Delta}, \quad H_{41} = \frac{-\det \begin{pmatrix} l_{11} & l_{12} & l_{14} & l_{13} \\ l_{21} & l_{22} & l_{24} & l_{23} \\ l_{41} & l_{42} & l_{44} & l_{43} \\ l_{51} & l_{52} & l_{54} & l_{53} \end{pmatrix}}{\Delta},$$

$$H_{42} = \frac{-\det \begin{pmatrix} l_{11} & l_{12} & l_{14} & l_{16} \\ l_{21} & l_{22} & l_{24} & l_{26} \\ l_{41} & l_{42} & l_{44} & l_{46} \\ l_{51} & l_{52} & l_{54} & l_{56} \end{pmatrix}}{\Delta}, \quad H_{43} = \frac{\det \begin{pmatrix} l_{11} & l_{12} & l_{14} & l_{19} \\ l_{21} & l_{22} & l_{24} & l_{29} \\ l_{41} & l_{42} & l_{44} & l_{49} \\ l_{51} & l_{52} & l_{54} & l_{59} \end{pmatrix}}{\Delta}.$$

$$\Delta = \det \begin{pmatrix} l_{11} & l_{12} & l_{14} & l_{15} \\ l_{21} & l_{22} & l_{24} & l_{25} \\ l_{41} & l_{42} & l_{44} & l_{45} \\ l_{51} & l_{52} & l_{54} & l_{55} \end{pmatrix}.$$

**Funding** Trường Đại học Công nghệ, Đại học Quốc Gia Hà Nội, CN22.11, Dinh Duc Nguyen.

## Declarations

**Conflict of interest** The authors declare no conflict of interest.

**Ethical approval** All authors certify that we have participated sufficiently in the work to take public responsibility for the content, including participation in the concept, design, analysis, writing, or revision of the manuscript. Furthermore, each author certifies that this material or similar material has not been and will not be submitted to or published in any other publication before its appearance in the Journal, if accepted—it will not be published elsewhere in the same form in English or in any other language, including electronically without the written consent of the copyright-holder.

## References

- Irie T, Yamada G, Tsujino M. Vibration and stability of a variable thickness annular plate subjected to a torque. *J Sound Vib.* 1982;85(2):277–85. [https://doi.org/10.1016/0022-460X\(82\)90522-3](https://doi.org/10.1016/0022-460X(82)90522-3).
- Efraim E, Eisenberger M. Exact vibration analysis of variable thickness thick annular isotropic and FGM plates. *J Sound Vib.* 2007;299(4):720–38. <https://doi.org/10.1016/j.jsv.2006.06.068>.
- Koiter WT, Elishakoff I, Li YW, Starnes JH. Buckling of an axially compressed cylindrical shell of variable thickness. *Int J Solids Struct.* 1994;31(6):797–805. [https://doi.org/10.1016/0020-7683\(94\)90078-7](https://doi.org/10.1016/0020-7683(94)90078-7).
- Nguyen HLT, Elishakoff I, Nguyen VT. Buckling under the external pressure of cylindrical shells with variable thickness. *Int J Solids Struct.* 2009;46(24):4163–8. <https://doi.org/10.1016/j.ijssolstr.2009.07.025>.
- Li YW, Elishakoff I, Starnes JH. Axial buckling of composite cylindrical shells with periodic thickness variation. *Comput Struct.* 1995;56(1):65–74. [https://doi.org/10.1016/0045-7949\(94\)00527-A](https://doi.org/10.1016/0045-7949(94)00527-A).
- Brar G, Hari Y, Williams D. Buckling of Axisymmetric Cylindrical Shells of Variable Thickness: Finite Difference Solution. Proceedings of the ASME 2007 Pressure Vessels and Piping Conference. San Antonio, Texas, USA. 2007;627–633. ASME. <https://doi.org/10.1115/PVP2007-26234>
- Chen Z, Yang L, Cao G, Guo W. Buckling of the axially compressed cylindrical shells with arbitrary axisymmetric thickness variation. *Thin Walled Struct.* 2012;60:38–45. <https://doi.org/10.1016/j.tws.2012.07.015>.
- Feng WZ, Chen ZP, Jiao P, Zhou F, Fan HG. Buckling of cylindrical shells with arbitrary circumferential thickness variations under external pressure. *J Mech.* 2017;33(1):55–64. <https://doi.org/10.1017/jmech.2016.59>.
- Zhou F, Chen Z, Fan H, Huang S. Analytical study on the buckling of cylindrical shells with stepwise variable thickness subjected to uniform external pressure. *Mech Adv Mater Struct.* 2016;23(10):1207–15. <https://doi.org/10.1080/15376494.2015.1068401>.
- Taati E, Fallah F, Ahmadian MT. Closed-form solution for free vibration of variable-thickness cylindrical shells rotating with a constant angular velocity. *Thin Walled Struct.* 2021;166:108062. <https://doi.org/10.1016/j.tws.2021.108062>.
- Duan WH, Koh CG. Axisymmetric transverse vibrations of circular cylindrical shells with variable thickness. *J Sound Vib.* 2008;317(3):1035–41. <https://doi.org/10.1016/j.jsv.2008.03.069>.
- Ganesan N, Sivasdas KR. Free vibration of cantilever circular cylindrical shells with variable thickness. *Comput Struct.* 1990;34(4):669–77. [https://doi.org/10.1016/0045-7949\(90\)90246-X](https://doi.org/10.1016/0045-7949(90)90246-X).
- Sivasdas KR, Ganesan N. Free vibration of circular cylindrical shells with axially varying thickness. *J Sound Vib.* 1991;147(1):73–85. [https://doi.org/10.1016/0022-460X\(91\)90684-C](https://doi.org/10.1016/0022-460X(91)90684-C).
- El-Kaabazi N, Kennedy D. Calculation of natural frequencies and vibration modes of variable thickness cylindrical shells using the Wittrick-Williams algorithm. *Computers Struct.* 2012;104–105:4–12. <https://doi.org/10.1016/j.compstruc.2012.03.011>.
- Viswanathan KK, Kim KS, Lee KH, Lee JH. Free vibration of layered circular cylindrical shells of variable thickness using spline function approximation. *Math Probl Eng.* 2010;28(6):1–14. <https://doi.org/10.1155/2010/547956>.
- Aksogan O, Sofiyev AH. Dynamic buckling of a cylindrical shell with variable thickness subject to a time-dependent external pressure varying as a power function of time. *J Sound Vib.* 2002;254(4):693–702. <https://doi.org/10.1006/jsvi.2001.4115>.
- Jia-chu X, Cheng W, Ren-huai L. Nonlinear stability of truncated shallow conical sandwich shell with variable thickness. *Appl Math Mech.* 2000;21(9):977–86. <https://doi.org/10.1007/BF02459306>.
- Xin-zhi W, Ming-jun H, Yong-gang Z, Kai-yuan Y. Nonlinear natural frequency of shallow conical shells with variable thickness. *Appl Math Mech.* 2005;26(3):277–82. <https://doi.org/10.1007/BF02440076>.
- Kalbaran Ö, Kurtaran H. Large displacement static analysis of composite elliptical panels of revolution having variable thickness and resting on winkler-pasternak elastic foundation. *Latin Am J Solids Struct.* 2019;16(9):1–26. <https://doi.org/10.1590/1679-78255842>.
- Nasrekani FM, Eipakchi H. Nonlinear analysis of cylindrical shells with varying thickness and moderately large deformation under nonuniform compressive pressure using the first-order shear deformation theory. *J Eng Mech.* 2015;141(5):04014153. [https://doi.org/10.1061/\(ASCE\)EM.1943-7889.0000875](https://doi.org/10.1061/(ASCE)EM.1943-7889.0000875).
- Eipakchi H, Nasrekani FM. Axisymmetric analysis of auxetic composite cylindrical shells with honeycomb core layer and variable thickness subjected to combined axial and non-uniform radial pressures. *Mech Adv Mater Struct.* 2022;29(12):1798–812. <https://doi.org/10.1080/15376494.2020.1841346>.
- Duc ND, Kim S-E, Vu TAT, Vu AM. Vibration and nonlinear dynamic analysis of variable thickness sandwich laminated

- composite panel in thermal environment. *J Sandw Struct Mater.* 2020;23(5):1541–70. <https://doi.org/10.1177/1099636219899402>.
23. Shariyat M, Alipour MM. Analytical bending and stress analysis of variable thickness FGM auxetic conical/cylindrical shells with general tractions. *Latin Am J Solids Struct.* 2017;14(5):805–43. <https://doi.org/10.1590/1679-78253413>.
  24. Khoshgoftar MJ. Second order shear deformation theory for functionally graded axisymmetric thick shell with variable thickness under non-uniform pressure. *Thin Walled Struct.* 2019;144:106286. <https://doi.org/10.1016/j.tws.2019.106286>.
  25. Khoshgoftar M, Mirzaali MJ, Rahimi G. Thermoelastic analysis of non-uniform pressurized functionally graded cylinder with variable thickness using first order shear deformation theory (FSDT) and perturbation method. *Chin J Mech Eng.* 2015;28(6):1149–56. <https://doi.org/10.3901/CJME.2015.0429.048>.
  26. Parhizkar Yaghoobi M, Ghannad M. An analytical solution for heat conduction of FGM cylinders with varying thickness subjected to non-uniform heat flux using a first-order temperature theory and perturbation technique. *Int Commun Heat Mass Transf.* 2020;116:104684. <https://doi.org/10.1016/j.icheatmasstransfer.2020.104684>.
  27. Kashkoli MD, Tahan KN, Nejad MZ. Thermomechanical creep analysis of FGM thick cylindrical pressure vessels with variable thickness. *Int J Appl Mech.* 2018;10(01):1850008. <https://doi.org/10.1142/S1758825118500084>.
  28. Saeedi S, Kholdi M, Loghman A, Ashrafi H, Arefi M. Axisymmetric thermoelastic analysis of long cylinder made of FGM reinforced by aluminum and silicone carbide using DQM. *Arch Civ Mech Eng.* 2022;22(1):48. <https://doi.org/10.1007/s43452-022-00376-x>.
  29. Behravan Rad A, Shariyat M. Thermo-magneto-elasticity analysis of variable thickness annular FGM plates with asymmetric shear and normal loads and non-uniform elastic foundations. *Arch Civil Mech Eng.* 2016;16(3):448–66. <https://doi.org/10.1016/j.acme.2016.02.006>.
  30. Hayati M, Atai AA. Multiobjective mechanical buckling optimization of variable thickness FG cylindrical shell with initial imperfection. *J Eng Appl Sci.* 2019;14(2):658–65. <https://doi.org/10.36478/jeasci.2019.658.665>.
  31. Minh PP, Duc ND. The effect of cracks on the stability of the functionally graded plates with variable-thickness using HSDT and phase-field theory. *Compos Part B.* 2019;175:107086. <https://doi.org/10.1016/j.compositesb.2019.107086>.
  32. Akbari Alashti R, Ahmadi SA. Buckling analysis of functionally graded thick cylindrical shells with variable thickness using DQM. *Arab J Sci Eng.* 2014;39(11):8121–33. <https://doi.org/10.1007/s13369-014-1356-4>.
  33. Kim J, Choe C, Hong K, Jong Y, Kim K. Free and forced vibration analysis of moderately thick functionally graded doubly curved shell of revolution by using a semi-analytical method. *Iran J Sci Technol Trans Mech Eng.* 2022. <https://doi.org/10.1007/s40997-022-00518-9>.
  34. Phu KV, Bich DH, Doan LX. Nonlinear forced vibration and dynamic buckling analysis for functionally graded cylindrical shells with variable thickness subjected to mechanical load. *Iran J Sci Technol Trans Mech Eng.* 2022;46(3):649–65. <https://doi.org/10.1007/s40997-021-00429-1>.
  35. Quoc TH, Huan DT, Phuong HT. Vibration characteristics of rotating functionally graded circular cylindrical shell with variable thickness under thermal environment. *Int J Press Vessels Pip.* 2021;193:104452. <https://doi.org/10.1016/j.ijpvp.2021.104452>.
  36. Miao X-Y, Li C-F, Jiang Y-L, Zhang Z-X. Free vibration analysis of three-layer thin cylindrical shell with variable thickness two-dimensional FGM middle layer under arbitrary boundary conditions. *J Sandwich Struct Mater.* 2021;24(2):973–1003. <https://doi.org/10.1177/10996362211020429>.
  37. Ahlawat N, Saini R. Vibration and buckling analysis of elastically supported Bi-directional FGM mindlin circular plates having variable thickness. *J Vib Eng Technol.* 2023. <https://doi.org/10.1007/s42417-023-00856-1>.
  38. Kurpa L, Shmatko T, Timchenko G. Nonlinear dynamic analysis of FGM sandwich shallow shells with variable thickness of layers. In: Altenbach H, Amabili M, Miklin YV, editors. *Nonlinear mechanics of complex structures: from theory to engineering applications.* Cham: Springer International Publishing; 2021. p. 57–74. [https://doi.org/10.1007/978-3-030-75890-5\\_4](https://doi.org/10.1007/978-3-030-75890-5_4).
  39. Stein M, McElman JA. Buckling of segments of toroidal shells. *AIAA J.* 1965;3(9):1704–9. <https://doi.org/10.2514/3.55185>.
  40. Oyesanya MO. Influence of extra terms on asymptotic analysis of imperfection sensitivity of toroidal shell segment with random imperfection. *Mech Res Commun.* 2005;32(4):444–53. <https://doi.org/10.1016/j.mechrescom.2005.02.006>.
  41. Weingarten VI, Veronda DR, Saghera SS. Buckling of segments of toroidal shells. *AIAA J.* 1973;11(10):1422–4. <https://doi.org/10.2514/3.6930>.
  42. Ninh DG, Bich DH. Nonlinear thermal vibration of eccentrically stiffened Ceramic-FGM-metal layer toroidal shell segments surrounded by elastic foundation. *Thin Walled Struct.* 2016;104:198–210. <https://doi.org/10.1016/j.tws.2016.03.018>.
  43. Duc ND, Vuong PM. Nonlinear vibration response of shear deformable FGM sandwich toroidal shell segments. *Mechanica.* 2022;57(5):1083–103. <https://doi.org/10.1007/s11012-021-01470-9>.
  44. Long VT, Tung HV. Mechanical buckling analysis of thick FGM toroidal shell segments with porosities using Reddy's higher order shear deformation theory. *Mech Adv Mater Struct.* 2021. <https://doi.org/10.1080/15376494.2021.1969606>.
  45. Thinh TI, Bich DH, Tu TM, Van Long N. Nonlinear analysis of buckling and postbuckling of functionally graded variable thickness toroidal shell segments based on improved Donnell shell theory. *Compos Struct.* 2020;243:112173. <https://doi.org/10.1016/j.compstruct.2020.112173>.
  46. Reddy JN, Liu CF. A higher-order shear deformation theory of laminated elastic shells. *Int J Eng Sci.* 1985;23(3):319–30. [https://doi.org/10.1016/0020-7225\(85\)90051-5](https://doi.org/10.1016/0020-7225(85)90051-5).

**Publisher's Note** Springer Nature remains neutral with regard to jurisdictional claims in published maps and institutional affiliations.

Springer Nature or its licensor (e.g. a society or other partner) holds exclusive rights to this article under a publishing agreement with the author(s) or other rightsholder(s); author self-archiving of the accepted manuscript version of this article is solely governed by the terms of such publishing agreement and applicable law.